

CropSuite v1.0 - A comprehensive open-source crop suitability model considering climate variability for climate impact assessment

F. Zabel¹, M. Knüttel¹, B. Poschlod²

¹Department of Environmental Sciences, University of Basel, 4056 Basel, Switzerland

²Center for Earth System Research and Sustainability, Universität Hamburg, 20144 Hamburg, Germany

Correspondence to: florian.zabel@unibas.ch

Abstract.

Increasing demand for agricultural land resources and changing climate conditions require for strategic land-use planning and the development of adaptation strategies. Therefore, information about the suitability of agricultural land is a ~~necessary~~ prerequisite. Current suitability approaches often focus on single crops, can only be applied regionally and usually neglect the impact of climate variability on crop suitability. Here, we introduce CropSuite, a new comprehensive and easy-to-use ~~open source~~ crop suitability model that ~~makes it possible~~ allows to overcome these shortcomings. ~~CropSuite uses a fuzzy logic approach and is based on the assumption of Liebig's law of the minimum.~~ It provides a graphical user interface (GUI) and a wide range of pre- and postprocessing options, including a tool for data analysis, which allows users to easily apply the model and analyze the results. Further, it includes a spatial downscaling approach for climate data, which allows for performing enables crop suitability analysis at very high spatial resolution. ~~CropSuite uses a fuzzy logic approach and is based on the assumption of Liebig's law of the minimum.~~ Several ~~An expandable number of environmental and socio-economic~~ factors that impact on crop suitability can flexibly be integrated into CropSuite by determining membership functions. CropSuite allows for the consideration of irrigated and rainfed agricultural systems, vernalization requirements for winter crops, lethal temperature thresholds, photoperiodic sensitivity and several other limitations for crop growth. The model endogenously calculates and outputs climate-, soil-, and crop suitability, the optimal sowing- and harvest dates, the potential for multiple cropping, the (most) limiting factor(s), as well as the recurrence rate of potential crop failures according to the inter-annual climate variability. In this study, we apply CropSuite for 48 crops at a spatial resolution of 30 arc seconds (1 km at the equator) for Africa. Thereby, we consider regionally important staple and cash crops that are usually understudied, such as coffee, cassava, banana, oil palm, cocoa, cowpea, groundnuts, mango, millet, papaya, rubber, sesame, sorghum, sugar cane, tobacco, and yams. We find that the consideration of climate variability for calculating crop suitability makes a significant difference

31 on suitable areas, but also affects optimal sowing dates, and multiple cropping potentials. The most vulnerable regions
32 for climate variability are identified in Somalia, Kenya, Ethiopia, South Africa, and the Maghreb countries. The results
33 provide valuable crop-specific information that can be further used for climate impact assessments, adaptation and land-
34 use planning at global, regional, or local scale. CropSuite is provided open source and could be of interest for model
35 developers, scientists, and a wide range of potential users and stakeholders, such as farmers, companies, GOs, and NGOs.

36

37 **Key Words: Agriculture, Africa, Optimal Sowing Dates, Multiple Cropping, Maize**

38 **1 Introduction**

39 Climate change poses major challenges for agricultural production and food security. With warming climate, agricultural
40 suitability changes and suitable areas shift towards higher latitudes (Franke et al., 2021; Zabel et al., 2014). Crop
41 suitability models allow for a quantitative evaluation of land for crop cultivation and can therefore assess how the
42 suitability of land changes with changing climate. Contrary to mechanistic crop models (Jägermeyr et al., 2021;
43 Jägermeyr et al., 2020; Müller et al., 2024), crop suitability models are based on empirical approaches but are less
44 computational intensive and thus allow for the consideration of more crops at higher spatial resolution (Zabel et al., 2014).

45 ThereforeAs a result, crop suitability models provide important insights for sustainable land-use planning and climate
46 change adaptation, e.g. through cultivar change or land-use change. Akpoti et al. (2019) give an overview of existing
47 crop suitability approaches. Most studies are applied at regional scale (Maleki et al., 2017; Bonfante et al., 2015; Ranjitkar
48 et al., 2016), while just a few global approaches exist (Akpoti et al., 2019). In addition, Mmost studies focus just on single
49 crops and do not cover a variety of different crops (Ramirez-Villegas et al., 2013; Akpoti et al., 2020). Particularly for
50 Africa, domestically consumed staple crops, such as yams and cassava are often overseen in current studies, due to minor
51 economic relevance, despite their regional importance for food security (Chapman et al., 2020; Chemura et al., 2024;
52 Van Zonneveld et al., 2023; Karl et al., 2024). So far, none of the existing approaches systematically considers the impact
53 of climate variability on crop suitability, which is a major shortcoming, since climate variability is expected to increase
54 with climate warming and has a strong impact on agriculture (Vogel et al., 2019; Goulart et al., 2021; Ipcc, 2021).

55 The aim of this study is to introduce the CropSuite model, which is based on the crop suitability approach developed by
56 Zabel et al. (2014) and has continuously been further developed by Cronin et al. (2020) and Schneider et al. (2022a). The
57 model has previously been applied globally for 23 crops for different climate scenarios (Zabel, 2022). The model applies
58 Liebig's law of the minimum, assuming that the scarcest resource limits the crop growth. andCropSuite is based on a
59 fuzzy logic approach where, in contrast to Boolean logic, the truth value of variables can be any real number between 0
60 and 1. In fuzzy logic, fuzzy sets consist of elements whose degrees of memberships are described by membership
61 functions (Zadeh L.A., 1965). In our approach, we apply fuzzy logic to create , which uses crop-specific membership
62 functions (Fig. 1) describing the abiotic crop requirements between 0 (not suitable) and 100 (highly suitable) according

63 to various climatic, soil, and topographic variables (Zabel et al., 2014). Using a value range between 0 and 100 (instead
64 of 0 and 1) enables the use of an 8-bit integer data type for the internal calculation and storage of the results, which allows
65 efficient use of memory and hard disk. This approach is adopted, fundamentally redesigned and expanded with the goal
66 to provide a comprehensive but easy-to-use and flexible open-source model that can be applied e.g. by scientists, farmers,
67 companies, national or international institutions, GOs, ~~or~~ and NGOs. Therefore, CropSuite is now completely
68 reprogrammed in Python and consists of a graphical user interface (GUI), as well as several pre-processing and analysis
69 tools, e.g. for selecting a simulation domain, statistically downscaling the climate data, interpolating the membership
70 functions and automatically analyzing and mapping the results. In addition, CropSuite is complemented with a new
71 approach to consider the impact of climate variability on crop suitability. It includes a user manual, which is provided
72 together with the source code (Knüttel and Zabel, 2024).

73 2 Methods and Data

74 For this study, we apply CropSuite for Africa at 30 arc seconds spatial resolution (approximately 1 km² at the equator)
75 with the goal to simulate relevant but often overseen crops for this continent (Van Zonneveld et al., 2023). Table 1 shows
76 the 48 crops, that have been parameterized and simulated with CropSuite.

77
78 **Table 1: List of 48 considered crops simulated with CropSuite.** Binomial names are given in brackets.

1. Alfalfa (<i>Medicago sativa</i>)	25. Olive (<i>Olea europaea</i>)
2. Arabica Coffee (<i>Coffea arabica</i>)	26. Onion (<i>Allium cepa</i>)
3. Avocado (<i>Persea americana</i>)	27. Papaya (<i>Carica papaya</i>)
4. Banana (<i>Musa spp.</i>)	28. Pea (<i>Pisum sativum</i>)
5. Barley (<i>Hordeum vulgare</i>)	29. Pineapple (<i>Ananas comosus</i>)
6. Beans (<i>Phaseolus vulgaris</i>)	30. Potato (<i>Solanum tuberosum</i>)
7. Cabbage (<i>Brassica oleracea</i>)	31. Rapeseed (<i>Brassica napus</i>)
8. Carrot (<i>Daucus carota</i>)	32. Rice (<i>Oryza sativa</i>)
9. Cashew (<i>Anacardium occidentale</i>)	33. Robusta Coffee (<i>Coffea canephora</i>)
10. Cassava (<i>Manihot esculenta</i>)	34. Rubber (<i>Hevea brasiliensis</i>)
11. Castor Bean (<i>Ricinus communis</i>)	35. Rye (<i>Secale cereale</i>)
12. Chickpea (<i>Cicer arietinum</i>)	36. Safflower (<i>Carthamus tinctorius</i>)
13. Citrus (<i>Citrus spp.</i>)	37. Sesame (<i>Sesamum indicum</i>)
14. Cocoa (<i>Theobroma cacao</i>)	38. Sorghum (<i>Sorghum bicolor</i>)
15. Coconut (<i>Cocos nucifera</i>)	39. Soy (<i>Glycine max</i>)
16. Cotton (<i>Gossypium hirsutum</i>)	40. Sugar Cane (<i>Saccharum officinarum</i>)
17. Cowpea (<i>Vigna unguiculata</i>)	41. Sunflower (<i>Helianthus annuus</i>)
18. Green Pepper (<i>Capsium annuum</i>)	42. Sweet Potato (<i>Ipomoea batatas</i>)
19. Groundnut (<i>Arachis hypogaea</i>)	43. Tea (<i>Camellia sinensis</i>)
20. Guava (<i>Psidium guajava</i>)	44. Tobacco (<i>Nicotiana glauca</i>)
21. Maize (<i>Zea mays</i>)	45. Tomato (<i>Solanum lycopersicum esculentum</i>)

22. Mango (<i>Mangifera indica</i>)	46. Watermelon (<i>Colocynthis citrullus</i>)
23. Millet (<i>Pennisetum americanum</i>)	47. Wheat (<i>Triticum aestivum</i>)
24. Oil Palm (<i>Elaeis guineensis</i>)	48. Yams (<i>Dioscorea</i>)

79

80 We simulate a 20-year time period from 1991 to 2010 using the [Climate Hazards group Infrared Precipitation with](#)
81 [Stations \(CHIRPS\) v2.0 daily data for precipitation](#) (Funk et al., 2015) and the [Climate Hazards Center Infrared](#)
82 [Temperature with Stations \(CHIRTS\) v1.0 data for temperature](#) (Funk et al., 2019; Verdin et al., 2020) [at 2.5 arc minutes](#)
83 [spatial resolution for Africa. Both data sets provide climatologies at daily to monthly resolution based on a combination](#)
84 [of satellite remote sensing and climate stations. They benefit from long-term geostationary satellite observations,](#)
85 [delivering consistent data since the 1980s at the quasi-global \(50°S-50°N\) scale.](#)

86 In addition, soil and terrain information is required. Table 2 gives an overview of the soil and terrain data used for this
87 study. Soil data is mainly based on [ISRIC SoilGrids](#) (Hengl et al., 2017), which has a spatial resolution of 250 m but is
88 also provided at 1000 m spatial resolution. This data is reprojected to WGS84 and spatially interpolated using nearest
89 neighbor to the spatial resolution of 30 arc seconds applied in this study. Base saturation, gypsum, and exchangeable
90 sodium content (ESP, sodicity) are taken from the WISE database at a spatial resolution of 30 arc seconds (Batjes, 2016).
91 For electric conductivity, the ISRIC Global Soil Salinity Map with a resolution of 250 m is used (Ivushkin et al., 2019).
92 In contrast to the harmonized world soil database (HWSD) (Fao et al., 2012), the ISRIC soil datasets do not contain a
93 layer for texture class. For this reason, the texture class is determined using the sand and clay layer of SoilGrids according
94 to the United States Department of Agriculture (USDA) triangular diagram of soil texture classes (Fao et al., 2012). For
95 soil depths greater than 200 cm up to 50 m, the ISRIC dataset on absolute depth to bedrock (Hengl et al., 2017), is
96 complemented with the dataset from Pelletier et al. (2016), which covers soil depths up to 200 cm.

97 Available soil layers can be weighted in CropSuite as required. The SoilGrids datasets provide information for six depths:
98 0-5 cm, 5-15 cm, 15-30 cm, 30-60 cm, 60-100 cm, and 100-200 cm (Hengl et al., 2017; Hengl et al., 2014). [According](#)
99 [to Sys et al. \(1991\), soil properties have different effects on crop suitability depending on the soil layer. Accordingly, we](#)
100 [use weighting factors as proposed by](#) ~~[According to the available information, we adjust the different layers according to](#)~~
101 ~~[the weighting factors \(see Table 2\) as suggested by Sys et al. \(1991\) \(see Table 2\). The different distribution of the soil](#)~~
102 ~~[depths between the SoilGrids data and the weighting factors by Sys et al. \(1991\) is taken into account by using a](#)~~
103 ~~[proportional weighting of the SoilGrids layers.](#)~~

104 Terrain data are taken from the Shuttle Radar Topography Mission (SRTM) data set (Farr et al., 2007), which are used
105 to calculate the slope at the applied spatial resolution. Please be aware that a coarser spatial resolution generally reduces
106 the slope, which could result in an underestimation of possible slope limitations in mountainous regions. A possible
107 terracing could remove the restriction due to the slope but usually terraces are too small to be considered at the aggregated
108 spatial resolution of 30 arc seconds of the SRTM data in this study.

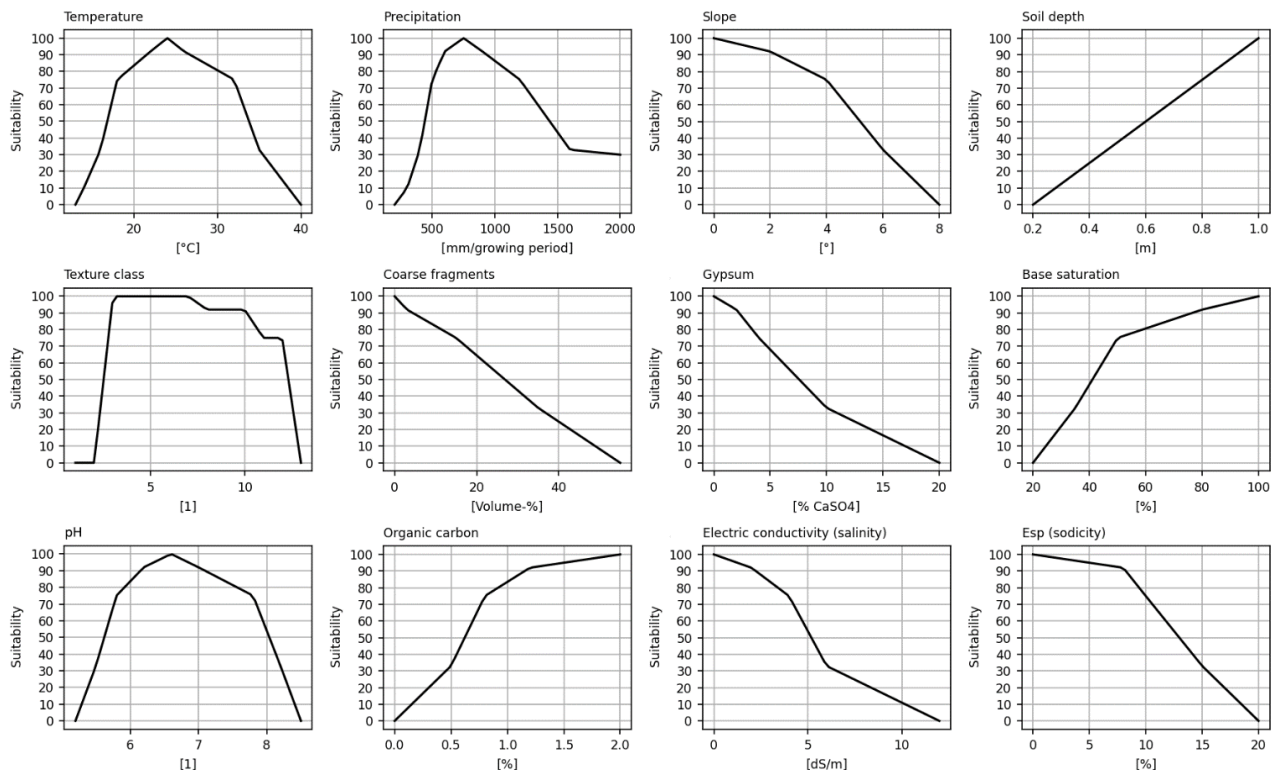
109

110 **Table 2: Soil and terrain data used in this study and the applied weighting of the different soil layers.**

Parameter	Source	Weighting
Base Saturation	ISRIC Harmonized Dataset of Derived Soil Properties for the World (WISE30sec)_(Batjes, 2016)	Only Top Soil
Coarse Fragments	ISRIC SoilGrids 250m_(Hengl et al., 2017)	0 - 25 cm: 2.0 25 - 50 cm: 1.5 50 - 75 cm: 1.0 75 - 100 cm: 0.75 100 - 125 cm: 0.5 125 - 150 cm: 0.25
Electric Conductivity	ISRIC Global Soil Salinity Map_(Ivushkin et al., 2019)	Only Top Soil
Gypsum Content	ISRIC Harmonized Dataset of Derived Soil Properties for the World (WISE30sec)_(Batjes, 2016)	Only Top Soil
Organic Carbon Content	ISRIC SoilGrids 250m_(Hengl et al., 2017)	0 - 25 cm: 2.0 25 - 50 cm: 1.5 50 - 75 cm: 1.0 75 - 100 cm: 0.75 100 - 125 cm: 0.5 125 - 150 cm: 0.25
Soil pH	ISRIC SoilGrids 250m_(Hengl et al., 2017)	0 - 5 cm: 0.33 5 - 15 cm: 0.33 15 - 30 cm: 0.33
Sodicity	ISRIC Harmonized Dataset of Derived Soil Properties for the World (WISE30sec) (Batjes, 2016)	Only Top Soil
Soil Depth	ISRIC SoilGrids 2017 (Soil Depth <= 200 cm)_(Hengl et al., 2017) Pelletier et al. 2017 Pelletier et al. (2016) (Soil Depth > 200 cm)	No Weighting
Texture Class	Texture Class calculated from ISRIC SoilGrids <250m Clay and Sand content (Hengl et al., 2017) according to USDA_(Fao et al., 2012)	0 - 25 cm: 2.0 25 - 50 cm: 1.5 50 - 75 cm: 1.0 75 - 100 cm: 0.75 100 - 125 cm: 0.5 125 - 150 cm: 0.25
Slope	SRTM aggregated to 30 arcsec_(Farr et al., 2007)	No Weighting

111
 112 Membership functions for temperature, precipitation, slope, soil depth, texture class, coarse fragments, gypsum, base
 113 saturation, pH, organic carbon, electric conductivity, sodicity (Fig. 1) are defined for the considered 48 crops relying on
 114 information from Sys et al. (1993), which provide membership functions for most of the considered crops. Additionally,
 115 data from the EcoCrop database, which provides crop [ecological](#) requirements for more than 2500 plant species
 116 (Fao, 2024), is used for Cowpea, Rye, and Yams. CropSuite in principle allows the flexible addition of any further
 117 membership function and dataset that is relevant [for the use case](#).

118 Nutrient deficits, such as nitrogen content are not considered in our approach, since according to our definition of crop
 119 suitability, they are not a decisive factor for the suitability of crops but rather depend on the crop management.
 120 Accordingly, we do not consider any soil tillage that can affect the soil properties, such as liming, which can influence
 121 the pH value.



122
 123 **Figure 1: Membership functions exemplarily for maize** with a growing cycle of 110 days for considered climatic (mean temperature
 124 over the growing cycle, total precipitation over the growing cycle), topographic (slope), and soil constraints (soil depth, texture class,
 125 coarse fragments, gypsum, base saturation, pH, organic carbon, salinity, sodicity).

126 Sys et al. (1993) uses a classification system with 6 classes, ranging from N2 as unsuitable to S0 as highly suitable. In
 127 this study, we dismiss the N1-classes due to a vague definition and differentiate three suitability classes, marginally,
 128 moderately, and highly suitable (Table 3).

129
 130 **Table 3: Crop suitability classification system as used in this study compared to Sys et al. (1993).**

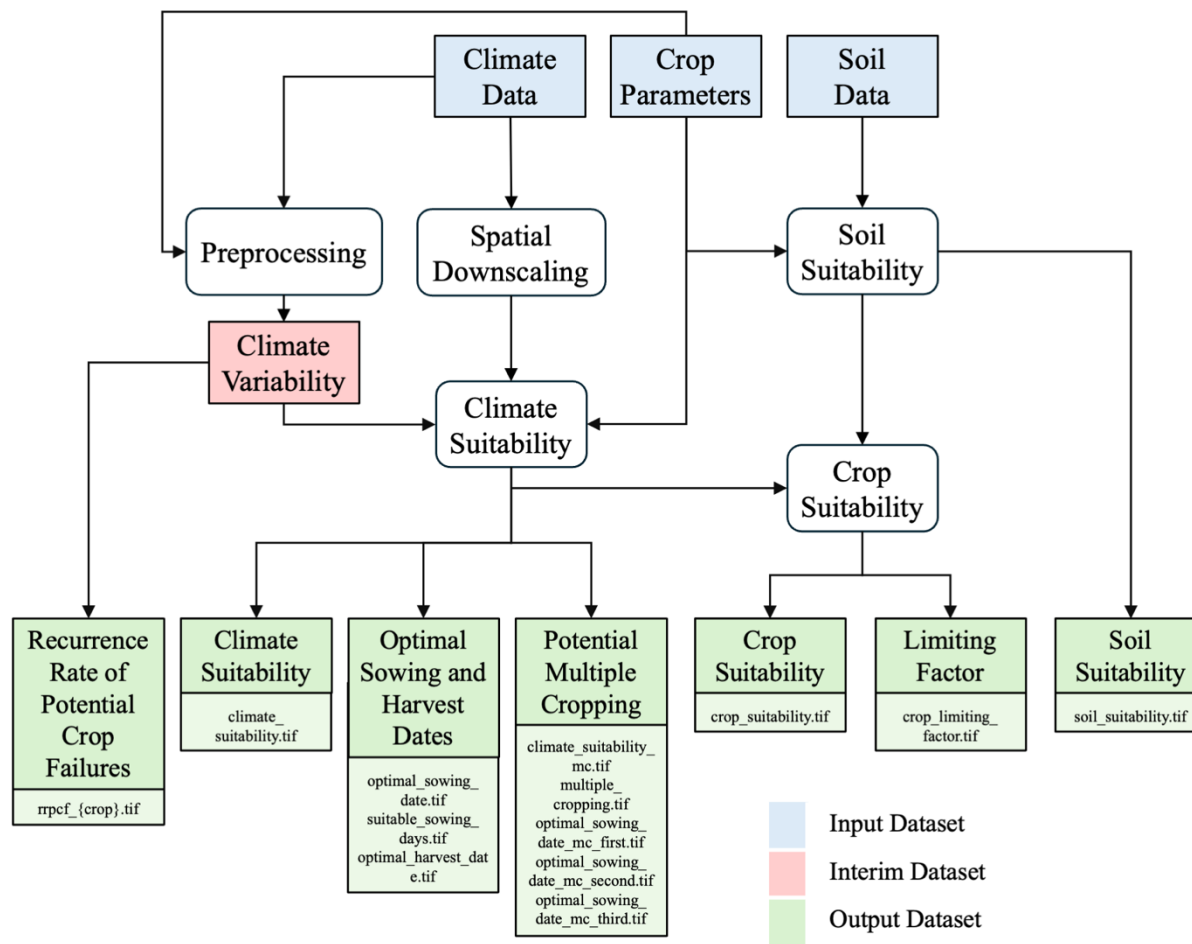
Suitability classes according to Sys et al.	Suitability range	Suitability classes used in this study
S0 (highly suitable)	100	75 – 100 (highly suitable)
S1 (very suitable)	80 – 99	
S2 (moderately suitable)	60 – 79	33 – 74 (moderately suitable)
S3 (marginally suitable)	40 – 59	1 – 32 (marginally suitable)
N1 (actually unsuitable and potentially suitable)	20 – 39	0 (unsuitable)
N2 (unsuitable)	0 - 19	

131 2.1 The CropSuite Model

132 Figure 2 shows the workflow and outputs of CropSuite, which first calculates a climate suitability (considering all climate
133 constraints) and then calculates a soil suitability (considering all soil and topography constraints). Both data records can
134 be output separately. Thereby, CropSuite applies Liebig’s law of the minimum, for both the climate and the soil suitability
135 by choosing the lowest suitability value between the different soil parameters and climate variables respectively. Finally,
136 the crop suitability is calculated from the combination of both climate and soil suitability by again following Liebig’s
137 law of the minimum, which means that the lowest suitability value between climate and soil suitability is chosen, since
138 it restricts overall crop suitability. The most limiting factor is identified as the parameter that imposes the greatest
139 constraint on growth for a specific crop. In addition, the magnitude of the constraint is output for each input factor.
140 Overall, CropSuite allows for a variety of outputs on optimal sowing- and harvest dates, suitable sowing days, multiple
141 cropping potentials, the limiting factor, and the recurrence rate of potential crop failures. [Output data format can be set
142 to GeoTIFF or NetCDF.](#)

143 CropSuite includes a pre-processing procedure which creates intermediate results for climate variability. Since climate
144 model data are usually available at relatively coarse spatial resolution, CropSuite has implemented a spatial downscaling
145 module for the climate data, which allows the model to be applied at very high spatial resolution from global to regional
146 to local scale. In this study, we apply a statistical downscaling to the climate data, refining the spatial resolution from 2.5
147 arc minutes to 30 arc seconds. In principle, the targeted spatial resolution can be set in CropSuite but is limited to the
148 available resolution of the additional input data, such as the soil data, whereas for the climate data, two different statistical
149 spatial downscaling methods are implemented requiring little computational effort. The first methodology is based on an
150 altitude regression for temperature (Marke et al., 2014), where the temperature gradients are extracted from the climate
151 model data itself via a moving window that can be set in size. Thereby, the extracted gradients must remain within the
152 natural boundaries for wet and dry adiabatic temperature gradients. The second downscaling methodology uses the
153 historical high-resolution spatial patterns for monthly temperature and precipitation taken from WorldClim at 30 arc
154 seconds spatial resolution (Fick and Hijmans, 2017). To downscale a coarse-resolution grid cell, all fine-resolution
155 WorldClim grid cells within the coarse-resolution cell are selected and aggregated per month. On this basis, additive
156 factors are calculated for temperature and multiplicative factors for precipitation separately for each month. Thereby the
157 sum (mean) of these additive (multiplicative) factors within the coarse-resolution cell amounts 0 (1). Considering the
158 monthly seasonality, these factors are applied to the coarse-resolution climate data, imprinting the spatial pattern of the
159 high-resolution reference data onto the coarse climate data [at daily time step](#). Both downscaling methods conserve mass
160 and energy from the climate input data by iteratively minimizing residuals over the simulation domain. For a more
161 advanced statistical downscaling to kilometer-scale, the expert user may apply more complex topographical downscaling
162 methods (Daly et al., 1994; Fiddes et al., 2022; Karger et al., 2023) or downscaling based on machine learning (Damiani
163 et al., 2024; Wang et al., 2021) outside of CropSuite. Furthermore, we do not recommend applying the implemented

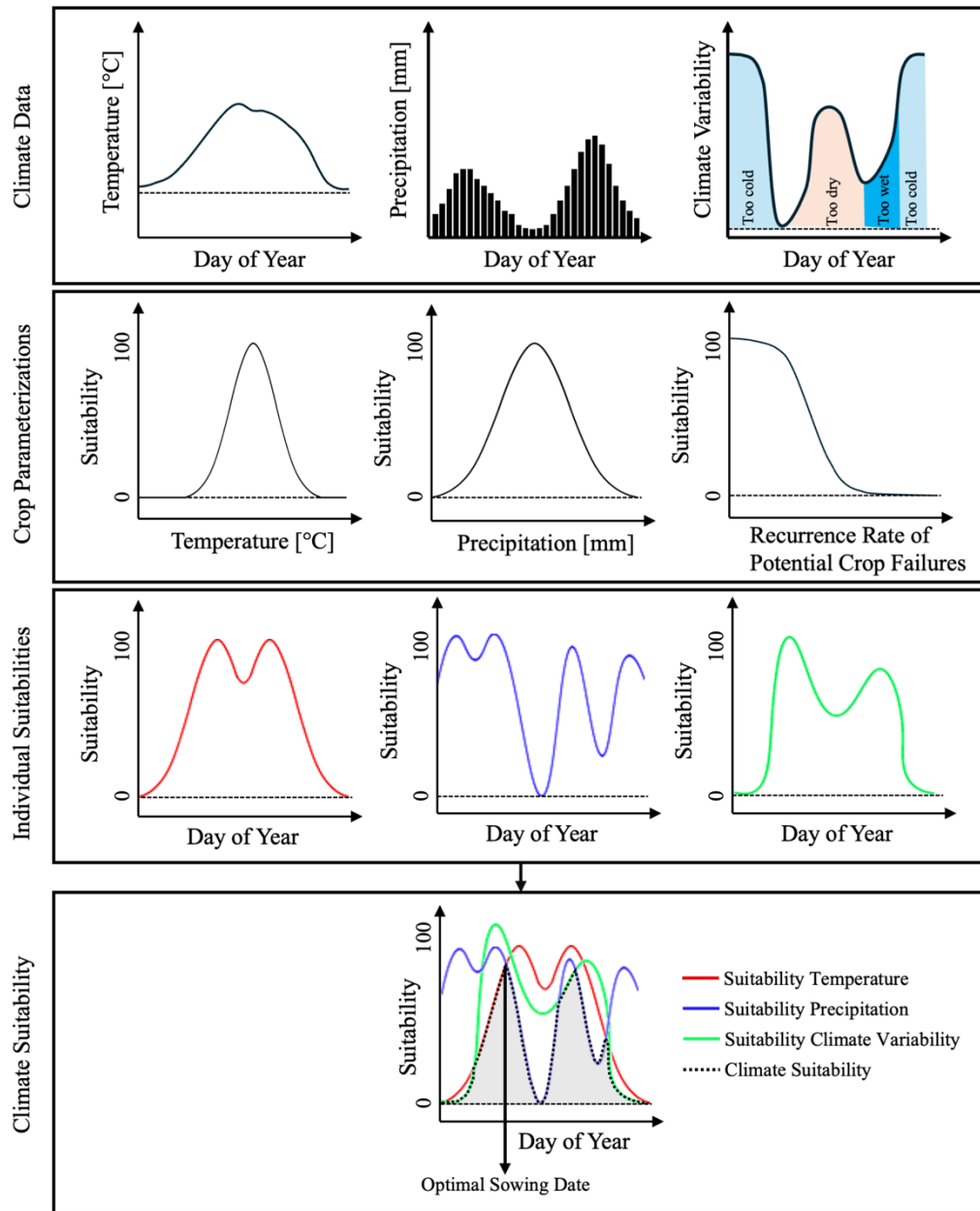
164 downscaling methods with high scaling factors from very coarse (hundreds of kilometers) to very high (single kilometer)
 165 resolution.



166
 167 **Figure 2: CropSuite workflow.** Input data in blue, intermediate results in red and output data in green. The processing steps are
 168 shown in white.

169 CropSuite requires daily climate data as an input for temperature and precipitation. As climate models tend to produce
 170 too many days with low-intensity precipitation called “drizzle bias” (Chen et al., 2021), days with aggregated daily
 171 precipitation values below 1 mm per day are considered to be dry days (Sun et al., 2006). This threshold can be set in the
 172 model. Both downscaled temperature and precipitation data and the calculated datasets for climate variability are used to
 173 calculate the climate suitability. Therefore, the crop-specific membership functions determine the suitability according
 174 to the average temperature, total precipitation and the recurrence rate of potential crop failures over the length of the
 175 growing cycle (time from sowing till maturity) for each day of year (DOY). Thereby, the suitability value for each DOY
 176 refers to the average conditions during the growing cycle from that DOY, which corresponds to the sowing date, until

177 maturity, determined by the length of the growing cycle which is set in the crop parameterization for each crop. For
178 perennial crops, the length of the growing cycle is set to 365 days. Climate suitability throughout the year is then identified
179 by selecting the minimum value (most limiting) of the three individual suitabilities for temperature, precipitation, and
180 climate variability. As shown in Fig. 3, the DOY with the highest climate suitability value over the year finally determines
181 DOY with the highest minimum of the three components throughout the year as shown in Fig. 3, thereby determining the
182 optimal sowing date for annual crops (optimal planting date for rice, which is not sown, but planted as a seedling in wet
183 rice cultivation). For perennial crops this is set to 1.



184

185 **Figure 3: Schematic illustration of the determination of climate suitability, the optimal sowing date and the limiting factor.** The
 186 input data shows the annual course of temperature, precipitation and the recurrence rate of potential crop failure, indicating whether it
 187 is too cold, too dry, or too wet. The plant-crop parameterizations show the membership functions for either temperature, precipitation,
 188 and climate variability resulting in the individual suitability values for each DOY for either temperature (red line), precipitation (blue
 189 line), and climate variability (green line).-Climate suitability throughout the year (black dashed line) results from the lowest of the
 190 three curves (most limiting) on any day. The highest value of climate suitability over the year finally determines the optimal sowing
 191 date. Finally, climate suitability and the optimal sowing date is determined by the highest minimum value of all three suitability curves.
 192 The limiting factor is the most constraining factor at this point.

193 For annual crops, CropSuite also calculates the potential for multiple harvests ~~of the same crop per year~~without
194 considering crop rotation. Between harvest and reseeding, we assume a certain time period (21 days in this study) for
195 field work and processing, which can be set flexibly in the model. Accordingly, all possible combinations of sowing dates
196 are tested with the aim to maximize climatic suitability to achieve the highest sum of climatic suitability within a year.
197 The optimal sowing dates are selected from the best sowing date combinations, resulting in one, two, or three sowing
198 dates per year. A multiple cropping layer is output that shows how often a crop can be harvested.

199 CropSuite distinguishes between rainfed and irrigated agricultural systems, which can be selected before starting the
200 simulation. For the irrigated case, precipitation is not considered as a constraining factor with consequences for all further
201 calculations, affecting e.g. the climate variability, the optimal sowing date, and the multiple cropping. For this study, we
202 separately simulated both, rainfed and irrigated options for all crops. In the post-processing, we combined both datasets
203 according to the irrigated areas dataset by Meier et al. (2018) (Fig. S1), which is available at 30 arc-seconds spatial
204 resolution.

205 For germination, crop-specific temperature and soil water ~~conditions~~ requirements can be set in the model. The latter can
206 be considered for rainfed conditions by defining a certain amount of precipitation within a certain period of time after
207 sowing.

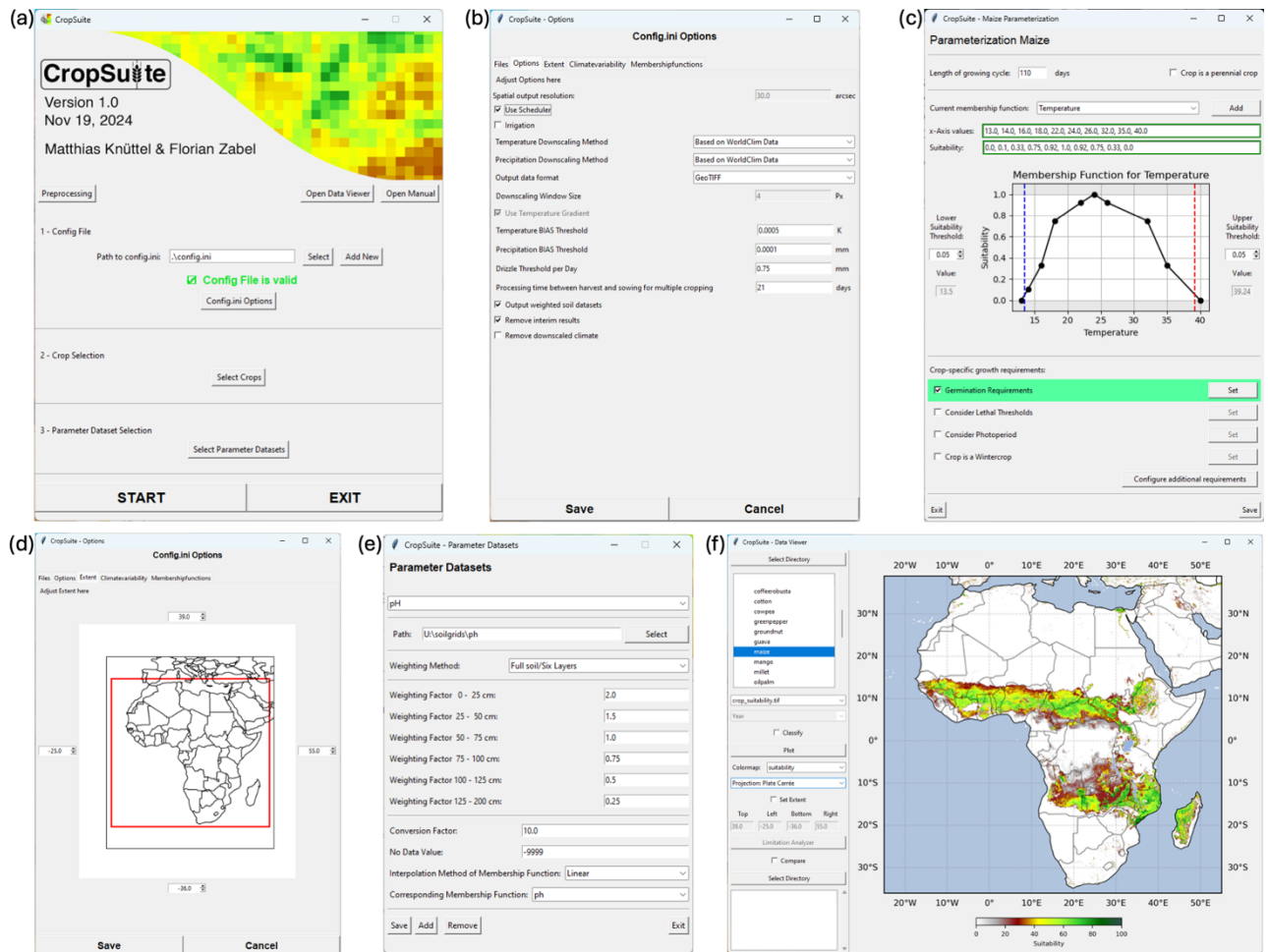
208 Some crops, such as soybean have a high photoperiodic sensitivity which can limit their suitability (Cober and Morrison,
209 2010; Abdulai et al., 2012). Therefore, crop-specific photoperiodic sensitivity can be considered in CropSuite by defining
210 a maximum and minimum day length in average over the growing cycle ~~can be considered in CropSuite~~.

211 Additional lethal climatic limitations ~~are can be~~ taken into account in CropSuite. We assume permafrost on areas with an
212 average annual temperature below 0° C, which is computed from the downscaled climate input data. A maximum lethal
213 temperature threshold of >40°C in average over the growing cycle is set for all crops (Asseng et al., 2021). In addition, a
214 minimum and maximum threshold for the lethal temperature over a certain consecutive number of days can be set in the
215 model crop-specifically. Further, the maximum number of consecutive dry days can be set dependent on the crop.

216 CropSuite allows for the consideration of vernalization requirements for winter crops. Therefore, crop-specific
217 temperature requirements with minimal and maximal temperature thresholds for a certain number of vernalization
218 effective days can be configured in the model. Accordingly, CropSuite simulates for each location, if and when these
219 vernalization requirements are fulfilled, which impacts on the length of the vernalization period and the optimal sowing
220 date. An offset of days from sowing to the start of the vernalization period can optionally be added.

221 A GUI is available for CropSuite that allows users to easily set-up the model, parameterize the crop requirements and the
222 membership functions (Fig. 4a-e), and to start the simulations. Further, new membership functions can be created, an
223 unlimited number of crop-specific requirements can be defined, and any additional data can be added, which can be
224 flexibly assigned to the defined membership functions (Fig. 4e). Moreover, new crops or crop varieties can be added.

225 The GUI also allows for the visualization, analysis and comparison of the results (Fig. 4f).



226
 227 **Figure 4: Graphical User Interface of CropSuite.** (a) shows the main screen, (b) exemplarily shows available model settings, (c)
 228 shows the available options for crop parameterizations exemplarily for maize, (d) shows the window to set-up the simulation domain,
 229 (e) exemplarily shows the set-up of a parameter dataset for soil pH, and (f) shows the integrated data viewer in CropSuite.

230 2.2 Climate Variability

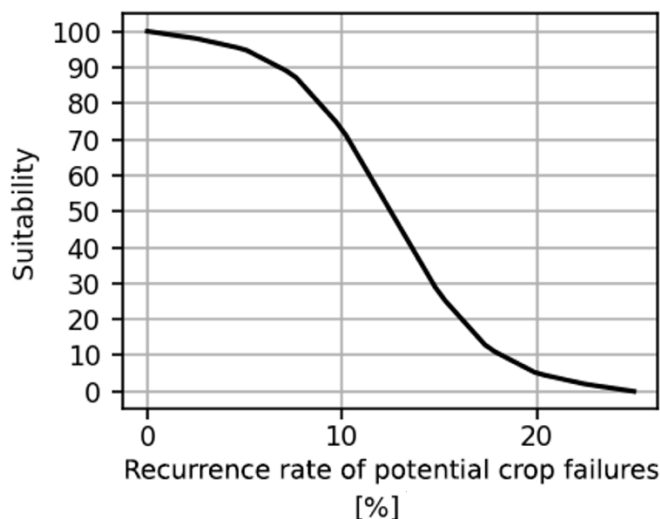
231 In addition to several improvements and redesigns, one of the most important advancements in CropSuite is the
 232 consideration of climate variability for the assessment of crop suitability. Usually, crop suitability models consider long-
 233 term climate averages, e.g. 10, 20 or 30-year periods and climatic trends that affect crop suitability (Ramirez-Villegas et
 234 al., 2013; Schneider et al., 2022b). They are not designed so simulate seasonal yields, as for instants mechanistic crop
 235 models do (Jägermeyr et al., 2021). However, existing crop suitability approaches may overestimate crop suitability when
 236 only long-term averages are considered, because a high climatic variability may result in a high frequency of unsuitable
 237 years, which would result in crop failures. This would however significantly increase the risk for farmers that require
 238 stable and plannable conditions. As a result, a farmer may conclude that the risk of crop failures due to unstable climate

239 conditions in a certain region is too high for being suitable for crop cultivation. As such, climate variability is not a purely
240 ecological limitation but depends on the socio-economic circumstances of how farmers deal with the risk of crop failure.
241 We developed an approach that allows for the consideration of climate variability, and thus the implicit integration of
242 socio-economic limitations in the suitability assessment of crops.

243 Therefore, we specify a crop-specific lower and upper threshold for temperature and precipitation. We recommend these
244 thresholds at between the higher and lower 5th and 10th and the 90th and 95th percentile suitability values of the crop-
245 specific membership function, respectively (Figs. 1, 4c). If the suitability of the membership function does not approach
246 0 at its high (low) limit, we recommend setting the threshold to the highest (lowest) value of the membership function.
247 This is the case for the wet limit of the precipitation membership function for maize (see Fig. 4c). For each year within a
248 given period of time (here we use 20-year time periods), it is tested and totaled, how often these thresholds exceed or fall
249 below during the growing cycle for all possible sowing dates (January 1st until December 31st). As a result, a variability
250 dataset is generated for each DOY, indicating the number of years in which at least either the temperature or the
251 precipitation exceeds or falls below the threshold values. The number of years is divided by the length of the time period
252 (here 20 years) to obtain the recurrence rate of potential crop failures. This data can be stored as a two-dimensional raster
253 file for perennial crops or as a three-dimensional raster file for non-perennial crops, with each of the 365 DOYs
254 representing the condition for the respective sowing day.

255 For rainfed agricultural systems, cases that are considered for climate variability include excessively high or low
256 temperatures and precipitation, while for irrigated agricultural systems, only excessively high or low temperatures and
257 excessively high precipitation are considered, to address potential water logging, plant diseases or root rotting. Due to
258 computational limitations, the preprocessing of the climate variability is carried out at the resolution of the input climate
259 data (2.5 arc minutes) and is further interpolated bilinearly to the output resolution of 30 arc seconds.

260 Finally, we introduce a membership function defining the impact of climate variability on crop suitability. As shown in
261 Fig. 5, a sigmoid is adopted for the course of the function. According to expert knowledge, we set this sigmoid function
262 in a way that it reduces suitability to 0 when the recurrence rate of potential crop failure is greater than once every 4 years
263 (25%). However, this function may be different in different parts of the world and different between crops (see
264 Discussion).



265

266

267

Figure 5: Membership function for climate variability showing the impact of the recurrence rate of potential crop failures on crop suitability. [The seasonal \$R_r\$ recurrence rate](#) is shown in percent.

268

3 Data Comparison Model evaluation

269

Crop suitability is difficult to validate or measure, nor is it equivalent to agricultural yields or production values. However, a comparison with other studies and data can provide valuable information and build confidence in the approach.

270

271

3.1 Comparison with Harvested Area

272

In principle, a crop should be suitable where it is already cultivated. ~~According~~According to this premise, we compare ~~the suitable area simulated with CropSuite with~~ the harvested areas ~~from from the global spatially-disaggregated crop production statistics data for 2020 (MapSPAM 2020 v1.0) produced by the International Food Policy Research Institute (IFPRI) using the Spatial Production Allocation Model (SPAM) (Ifpri, 2024). MapSPAM 2020 (Ifpri, 2024) with the suitable area from our simulation~~The CropSuite results for Africa ~~considering climate variability and are combined for irrigated and rainfed areas according to~~ Meier et al. (2018)~~from our simulation results for Africa~~. While MapSPAM relates to the year 2020, our simulations refer to the ~~1990~~1991-2010 time period, which could be a source of uncertainty. Nevertheless, we used MapSPAM 2020 ~~instead of other available versions of MapSPAM~~, since it includes 32 crops from our investigation ~~and is the latest released version of MapSPAM that was created with a special focus on Africa. A comparison between CropSuite and different MapSPAM versions is shown exemplarily for maize in Fig. S32, revealing a considerably better fit with CropSuite in the MapSPAM 2020 version.~~ For comparison, harvested areas below 10 ha per pixel are excluded from the calculation and the high spatial resolution of the CropSuite model output is resampled to the same spatial resolution (5 arc minutes) than the MapSPAM 2020 data.

273

274

275

276

277

278

279

280

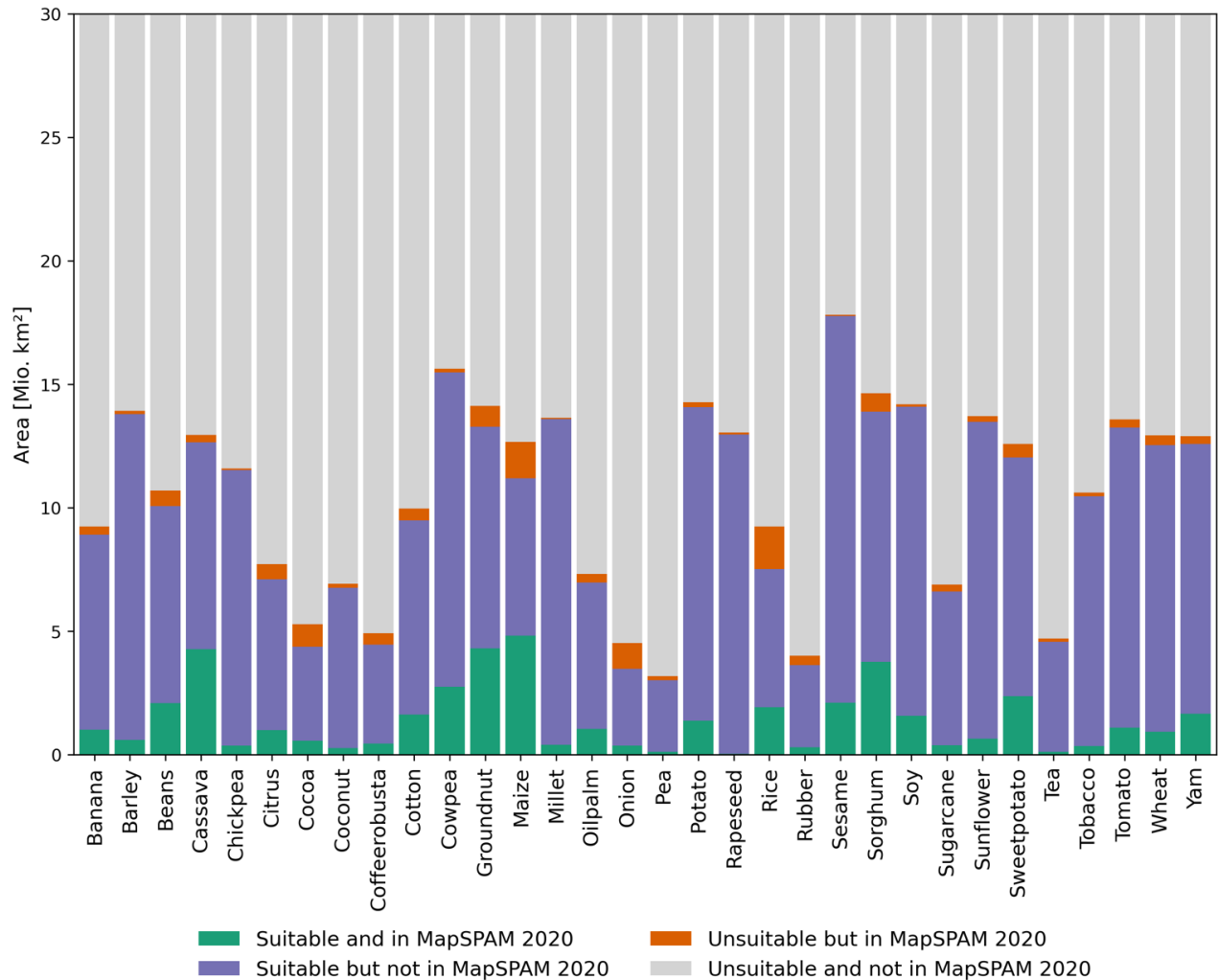
281

282

283

284

285 Figure 6 depicts the results of this analysis for all crops, where green and ~~blue-purple~~ bars represent areas that are suitable,
286 while ~~red-orange~~ and green areas ~~indicate-represent~~ harvested areas in MapSPAM. ~~Purple bars indicate suitable areas that~~
287 ~~are currently not used by the respective crop.~~-While green areas are also identified as being suitable in our approach, ~~red~~
288 ~~orange~~ areas are ~~harvested areas according to MapSPAM but~~ not suitable ~~according to~~ CropSuite ~~despite the respective~~
289 ~~crop is harvested according to MapSPAM.~~ -Crops with the largest mismatching areas are rice, maize, and onion (Fig. 6).
290 ~~Considering the ratio of red to green areas in Fig. 6, m~~Most crops show a small proportion of ~~mismatch~~~~orange to green~~
291 ~~areas~~, except for onions, ~~rapeseed, cocoa, peariee~~, rubber, ~~eeeee, and tea~~, coffee, and rice (Fig. S23). -This can have
292 various causes, such as data uncertainty of climate, soil and irrigation data (Avellan et al., 2012), incorrect membership
293 functions, the use of different crop varieties, or an incorrect localization of the cultivation areas in MapSPAM due to high
294 uncertainties in the underlying national statistical data, especially in African countries (Yu et al., 2020), or applied crop
295 management practices that could level out ecological limitations.



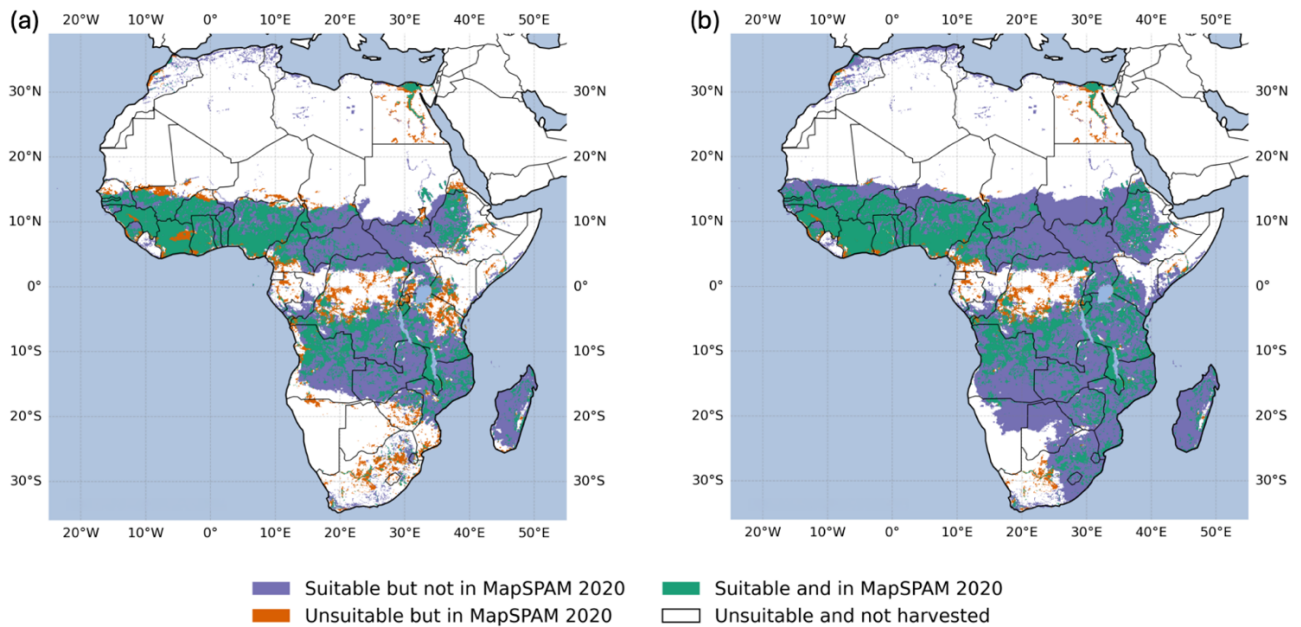
296

297 **Figure 6: Comparison of CropSuite with MapSPAM 2020 for all matching crops. CropSuite results combine irrigated and rainfed**
 298 **areas according to Meier et al. (2018) and consider climate variability.** Areas on which the respective crop is harvested according to
 299 MapSPAM and which are suitable according to CropSuite are shown in green, areas that are suitable but on which the crop is not
 300 harvested are shown in blue-purple. Areas that are not unsuitable but are harvested according to MapSPAM are shown in red-orange,
 301 while unsuitable areas that are not harvested according to MapSPAM are shown in gray.-

302 Figure 7a shows the spatial comparison between crop suitability and harvested areas for maize. Areas where maize is
 303 harvested according to MapSPAM, although CropSuite has identified these areas as unsuitable, are found mainly in
 304 Egypt, the northern Sahel, the Congo Basin, as well as parts of Cameroon, Gabon, Kenya, Tanzania, Zimbabwe and
 305 South Africa. Figure 7b shows the comparison ignoring the impact of climate variability on crop suitability. Disregarding
 306 climate variability results in large (blue) areas, which are considered suitable but are no harvest areas according to
 307 MapSPAM, especially along the dry belts (15°N and 20°S). Our approach considering climate variability (Fig. 7a)
 308 reduces these blue areas, but induces some mismatches, where MapSPAM indicates harvested areas and CropSuite shows

309 no suitability (red areas). We find that the mismatching areas along the dry belts (including the Sahel) and in eastern
310 Africa (Tanzania, Kenya) are often associated with limits due to climate variability. This indicates that the thresholds for
311 climate variability (section 2.2) and the membership function (Fig. 5) might be parameterized slightly too exclusive.
312 However, some of these regions might be used as cropland by smallholders or subsistence farmers despite the high risk
313 of crop failures.

314 While in the inner tropics, the reason for limited crop suitability can primarily be attributed to soil acidity (pH), indicating
315 possible uncertainties with used SoilGrids dataset, differences in Egypt mainly result from discrepancies according to
316 different assumptions on irrigated areas.



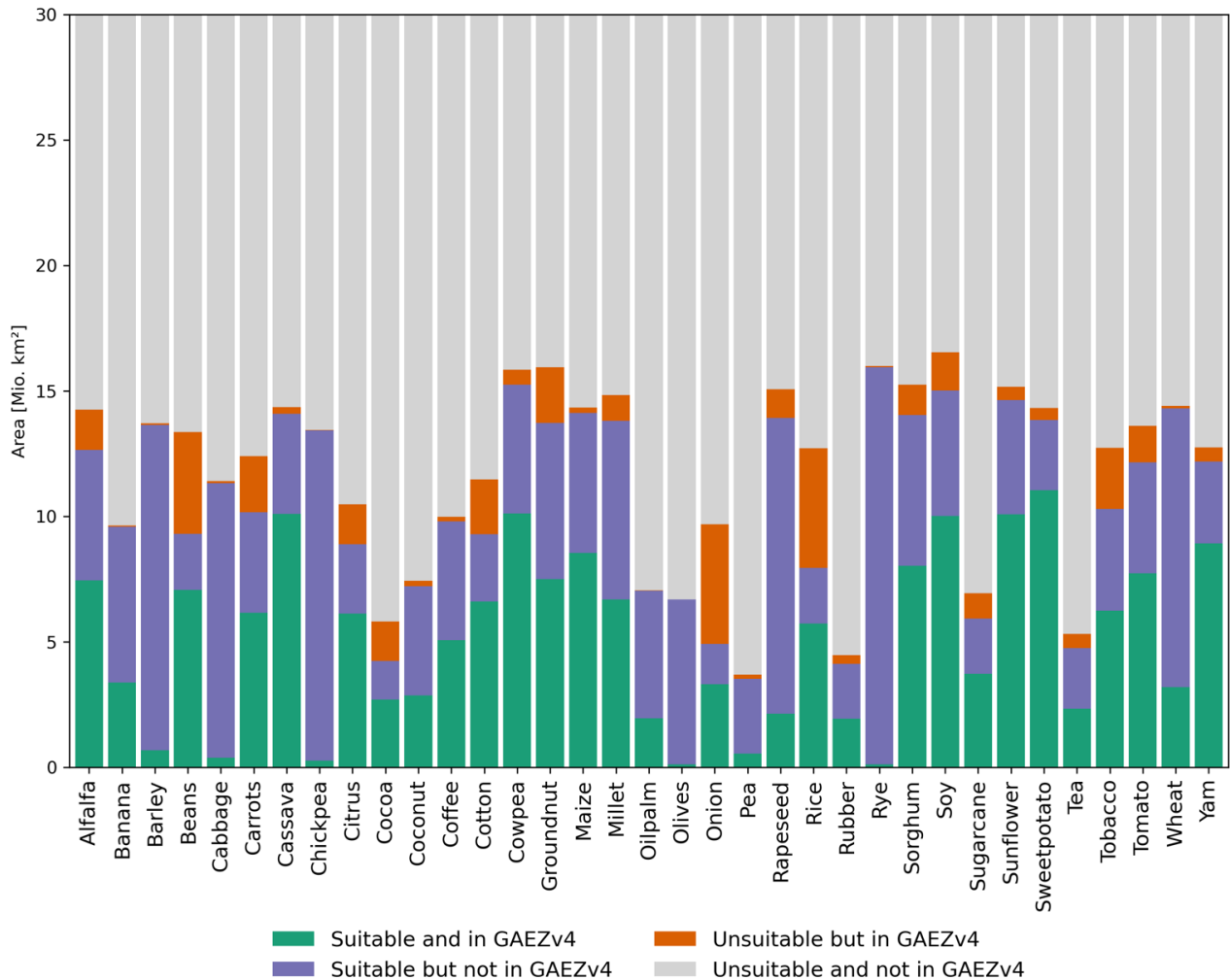
317
318 **Figure 7: Comparison of CropSuite with MapSPAM 2020 for maize.** (a) shows the comparison with consideration of climate
319 variability in CropSuite, while climate variability is not considered in (b). Areas on which the respective crop is harvested according
320 to MapSPAM and which are suitable according to CropSuite are shown in green, areas that are suitable but on which the crop is not
321 harvested are shown in blue. Areas that are not suitable but are harvested according to MapSPAM are shown in red. Unsuitable areas
322 that are not harvested according to MapSPAM are shown in white. (a) shows the comparison with consideration of climate variability
323 in CropSuite, while climate variability is not considered in (b).

324 3.2 Comparison with GAEZ

325 A state-of-the-art agroclimate-edaphic suitability assessment for crops is provided by the Global Agro-Ecological Zones
326 (GAEZ) v4.-(Fischer et al., 2021). For comparison with CropSuite, the suitability range of the GAEZ data we used GAEZ
327 data for the time period 1981-2010 for high input level, rainfed conditions and the option 'all land in grid cell'. The high
328 input level refers to advanced management assumptions (fully mechanized, optimum application of nutrients and
329 chemical pest, disease and weed control) (Fischer et al., 2021), which correspond best to the assumptions made in
330 CropSuite for this study. The suitability range of the GAEZ data is transformed to the classification system as shown in

331 Table 3. ~~In addition,~~ The CropSuite data for rainfed conditions is resampled (using the average) to the same spatial
332 resolution of 5 arc minutes than the GAEZ data. For this comparison, we use CropSuite data without climate variability,
333 since the GAEZ approach does not consider climate variability as well. Coffee was compared against the best type of
334 robusta and arabica, as done in the GAEZ data (Fischer et al., 2021).

335 Overall, there are large overlaps between the GAEZ and CropSuite (Fig. 8). Generally, CropSuite identifies larger suitable
336 areas than GAEZ for Africa (purple bar in Fig. 8), particularly for barley, cabbage, chickpea, rapeseed, rye and wheat. A
337 main reason for differences may be due to different underlying soil data, GAEZ uses the HWSO while CropSuite uses
338 the SoilGrids data. As an example, we found abrupt changes in the GAEZ results, especially between borders (e.g.
339 between Angola and Zambia), which follows patterns of the underlying HWSO, which is a known issue (Dewitte et al.,
340 2013). The consideration of climate variability in CropSuite mainly results in larger areas that are unsuitable in CropSuite
341 but still suitable in GAEZv4 (orange bars) (Fig. S4).



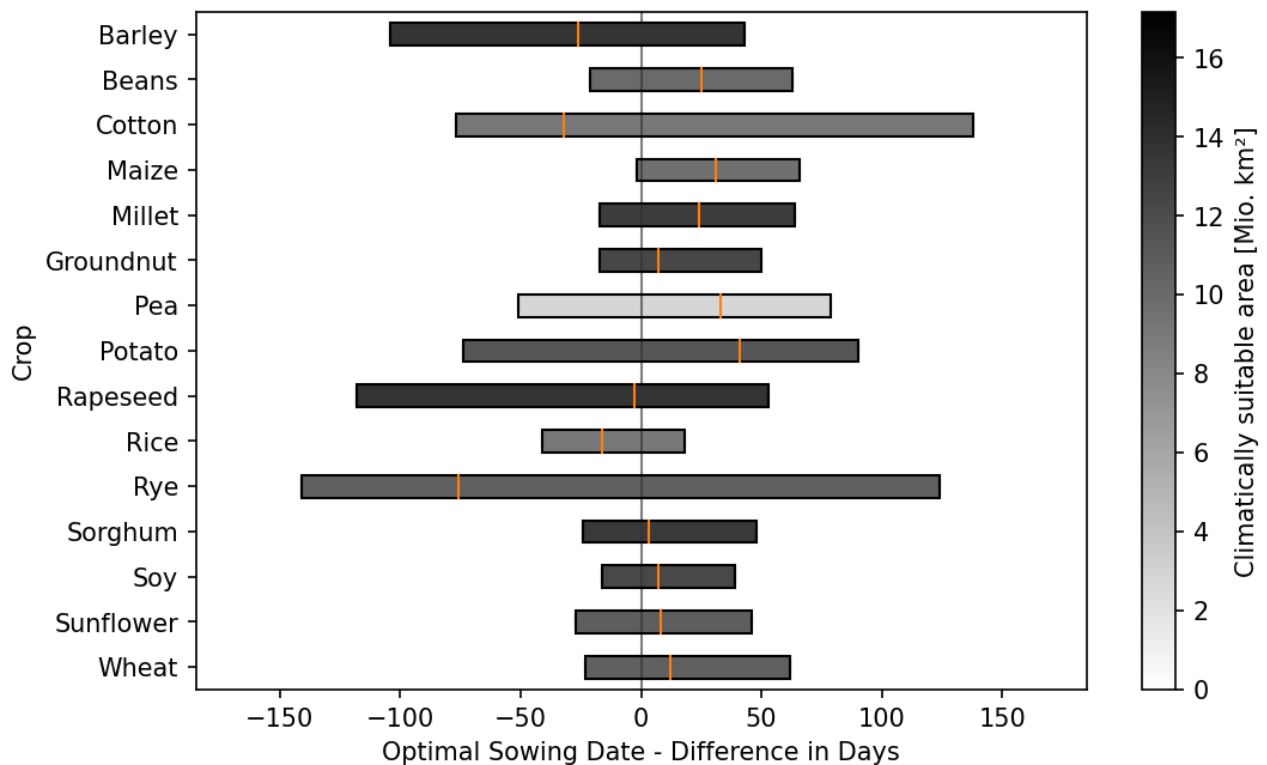
342

343 **Figure 8: Comparison between CropSuite and GAEZv4 suitability data for all matching crops.** CropSuite results are shown
 344 without consideration of climate variability. Areas that are suitable in both data, CropSuite and GAEZv4 are shown in green, areas
 345 suitable in CropSuite but not suitable in GAEZv4 are shown in purple. Unsuitable area in CropSuite that is suitable in GAEZv4 is
 346 shown in orange. Areas that are unsuitable in both data are shown in gray.

347 **3.3 Comparison of Optimal Sowing Dates with the GGCM Crop Calendar**

348 Another method of validation involves comparing the optimal sowing dates computed with CropSuite with the ~~GGCM~~
 349 crop calendar from the Global Gridded Crop Model Intercomparison (GGCMI), which is available globally for a variety
 350 of different crops at half degree spatial resolution (Jägermeyr et al., 2021). Figure 9 illustrates the average differences of
 351 the sowing dates across Africa, averaged for the matching crops between the two datasets. The ~~analysis-comparison~~ is
 352 performed at a spatial resolution of 30 arc seconds (Fig. 9) and at half degree resolution (see Fig. S5). For the high spatial
 353 resolution, the GGCMI data are bilinearly-interpolated to 30 arc seconds -using nearest neighbor- and then compared

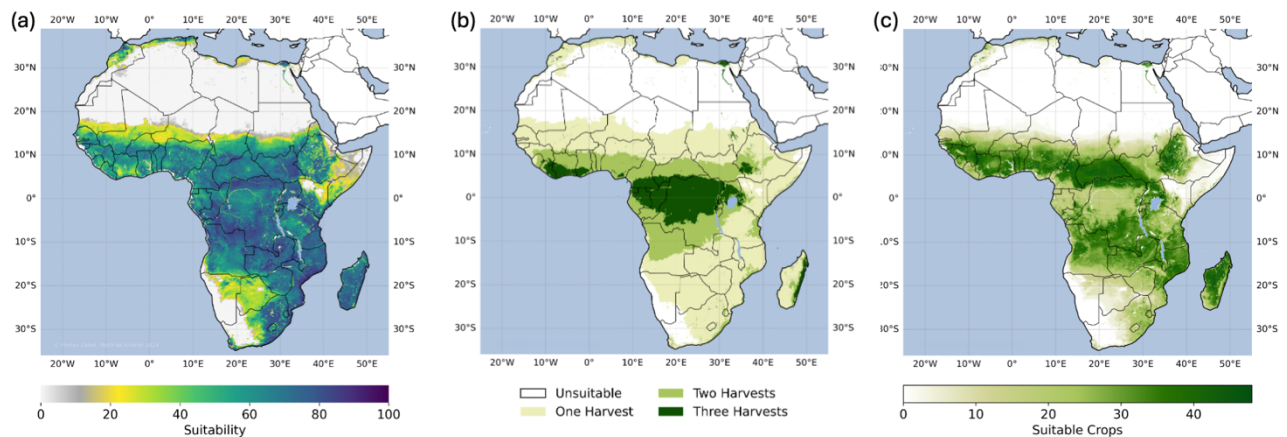
354 with the CropSuite data. Unlike CropSuite, which displays the optimal sowing date, the GGCM data show the actual
 355 sowing date based on interpolated-extrapolated statistics. Thus, there might be differences between the optimal and actual
 356 sowing dates. It must also be considered that the GGCM crop calendar is based on statistics that apply to discrete areas
 357 at relatively coarse half degree spatial resolution, while CropSuite was simulated at a pixel accuracy of 30 arc seconds
 358 spatial resolution. In fact, the median differences are mostly within one month of the GGCM crop calendar, which
 359 generally indicates a high agreement. Generally, we found that a greater distance to the equator potentially increased the
 360 discrepancy between the two data. As an example, in tropical climates with occurring dry and rainy seasons, a shift from
 361 one rainy season to another rainy season might result in a greater discrepancy. Also, we found that the distribution of
 362 sowing dates over the year was less concentrated in CropSuite, which could be a result of the higher spatial resolution
 363 (see Fig. S6). At the coarse resolution, the difference between the two datasets is less and the spread is smaller (Fig. S55).
 364



365
 366 **Figure 9: Comparison of the optimal sowing dates of CropSuite with the actual sowing dates of the GGCM crop calendars.**
 367 The area-weighted shift of the sowing date in days is shown for all matching crops. Negative values mean an earlier sowing date in
 368 CropSuite, positive values mean a later sowing date in CropSuite compared to the GGCM Crop Calendar. The bars show the 5th and
 369 95th percentile, the orange marker shows the median. The color of the bars indicates the climatically suitable area for the whole of
 370 Africa. Irrigated areas are considered according to Meier et al. (2018). The comparison is performed at 30 arc seconds spatial resolution
 371 for both datasets.

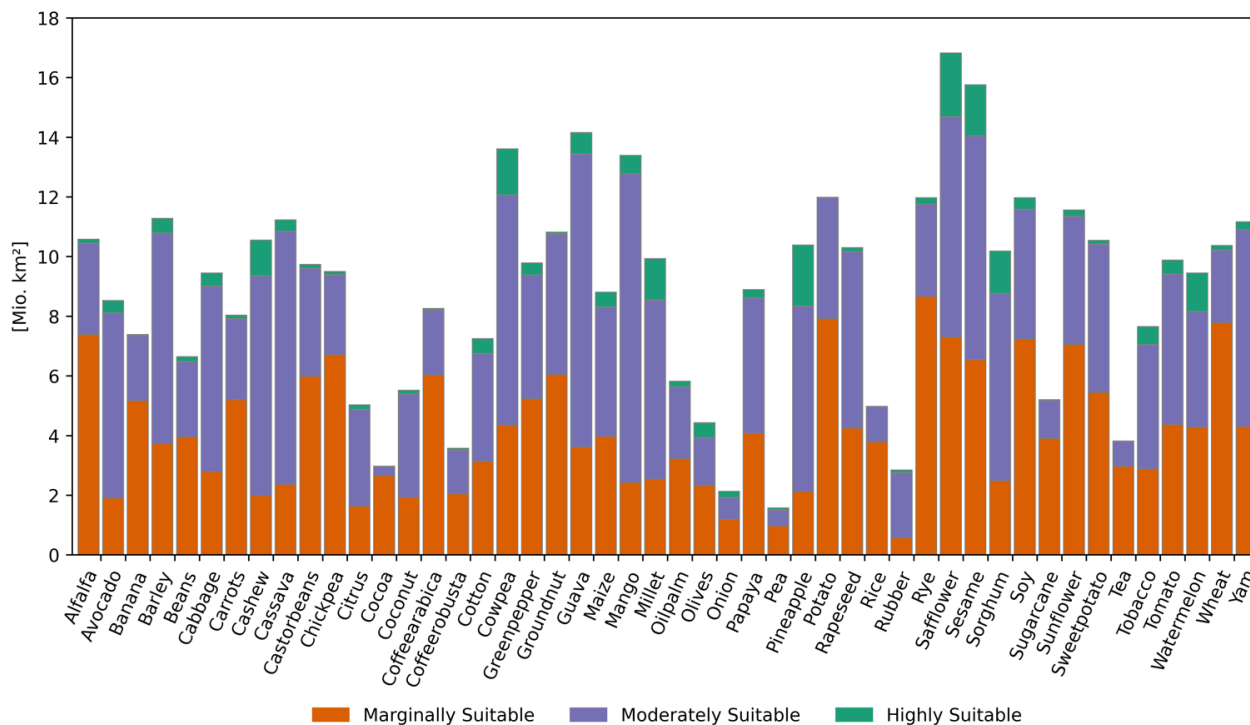
372 4 Simulation Results

373 Crop suitability is simulated for historical climate conditions (1991-2010) for rainfed and irrigated conditions. Figure 10a
374 illustrates the overall crop suitability, showing for each location the value for the most suitable of all considered crops.
375 Irrigation is considered according to the currently irrigated areas for Africa (Meier et al., 2018), such as along the Nile
376 river in Egypt (see Fig. S1 for irrigated areas in Africa). In total for Africa, 5.7 million km² are highly suitable, 10.6
377 million km² are moderately suitable, 3.3 million km² are marginally suitable and 10.4 million km² are not suitable for
378 crop cultivation. Mainly between 10° N and 10° S, a high potential for multiple cropping exists with the possibility of
379 two or three harvests per year (Fig. 10b). Looking at the number of crops suitable for cultivation (Fig. 10c), a large
380 proportion of the considered crops can grow particularly along the wet savannahs, which gives these regions plenty of
381 opportunities for cultivation. In contrast, only a few crops are suitable for the inner tropics and the dry savannahs, which
382 limits the possibilities for switching between culturescrops.



383
384 **Figure 10: (a) Overall crop suitability, (b) potential multiple cropping, and (c) number of suitable crops under historical climate**
385 **conditions from 1991 to 2010.** Irrigated areas are considered according to Meier et al. (2018). The overall crop suitability (a) and the
386 potential multiple cropping (b) are each shown for the most suitable crop at each location. The maximal number of suitable crops
387 results from the number of 48 considered crops (see Table 1). Figure 10a is shown with different colormap in the supplement (Fig.
388 S7).

389 Figure 11 shows the suitable area for each of the simulated crops for Africa. The five crops with the largest suitable areas
390 in Africa are safflower (16.82 mio km²), sesame (15.76), guava (14.15), cowpea (13.61), and mango (13.39).



391

392

393

Figure 11: Marginally, moderately and highly suitable areas for all 48 crops under historical climate conditions from 1991 to 2010 for Africa. Suitability classes are chosen according to Table 3. Irrigated areas are considered according to Meier et al. (2018).

394

Figure 12a exemplarily shows the crop suitability simulated for maize. The maps for all crops are provided via Zenodo

395

(see Data Availability). Maize is highly suitable along a strip of the 10° N and the 20° S parallel as well as large parts of

396

Mozambique and Madagascar. In total, 0.49 million km² are highly suitable, 4.34 million km² are moderately suitable,

397

3.97 million km² are marginally suitable and 21.23 million km² are unsuitable.

398

The optimal sowing date for single cropping (Fig. 12b) for maize shifts with latitude from the northern hemisphere across

399

the equator to the southern hemisphere. Figure 12c shows the potential number of potential harvests per year for maize.

400

Climate conditions allow up to two harvests per year in some parts of Congo and Cameroon and in the irrigated areas e.g.

401

along the Nile river. Optimal sowing dates for first and second sowing on areas suitable for multiple cropping are shown

402

in Fig. S268.

403

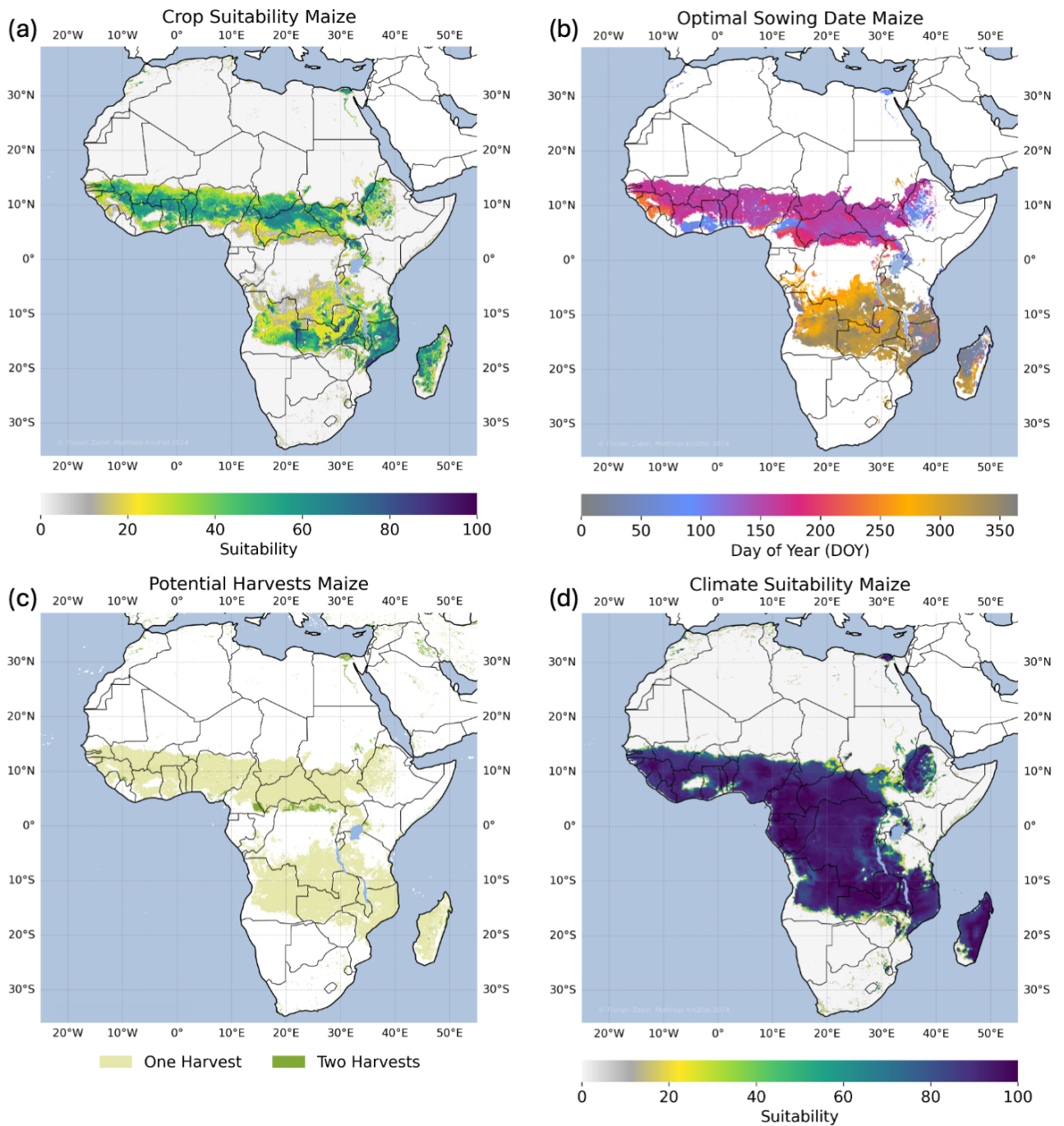
Figure 12d shows the climate suitability for maize, which just considers climatic constraints for the suitability of maize.

404

In comparison to the crop suitability map (Fig. 12a), more areas are suitable and suitability is substantially higher, where

405

if soil and topography are not considered and therefore do not limit or reduce crop suitability.



406

407

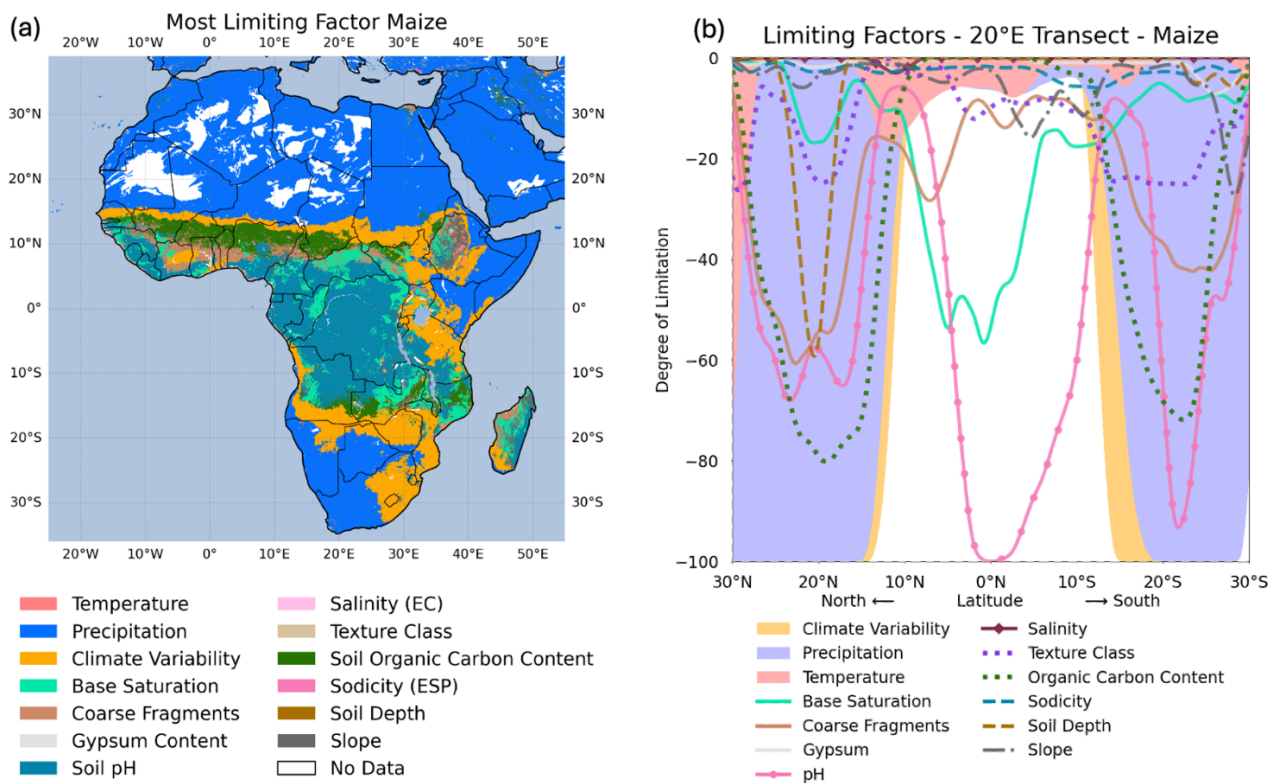
408

409

Figure 12: (a) Crop suitability, (b) optimal sowing date for single cropping, (c) potential multiple cropping, and (d) climate suitability for maize under historical climate conditions from 1991 to 2010. Irrigated areas are considered according to Meier et al. (2018). [Figure 12a is shown with different colormap in the supplement \(Fig. S9\).](#)

410 The most limiting factor is shown in Fig. 13a. While low precipitation prevents maize from being suitable in large parts
 411 of Africa in the arid deserts, soil is predominantly restricting suitability in tropical regions. Particularly pH is the most
 412 limiting factor in the humid tropics, such as the Congo Basin, where soils are too acid for growing maize. A large band
 413 along the drylands highlights regions where inter-annual climate variability is most limiting maize suitability (in orange,
 414 Fig. 13a). Here, climate conditions are unstable for maize cultivation, and the recurrence rate of potential crop failures is
 415 larger than 25% (every fourth year). For maize, climate variability is limiting crop suitability on 4.4 million km² for
 416 Africa (Fig 13a).

417 Figure 13b shows the degree of limitation for all considered climate, soil and terrain factors along a transect following
 418 the 20° E from North to South. In the Sahara, several factors, including temperature, organic carbon content, and soil pH,
 419 are not in an optimal range, while precipitation and the climate variability are the most limiting (note that climate
 420 variability is by definition a limiting factor if precipitation and/or temperature are limiting factors). Due to the unfavorable
 421 soil conditions, irrigation would only slightly improve maize suitability here. Between 15° N and 5° N, the limitations of
 422 all factors are relatively low. Here, coarse fragments and base saturation are most limiting. The tropical areas along the
 423 transect between 5° N and 10° S are mainly constrained by soil pH. Accordingly, soil management or practices that
 424 increase pH in these regions would have a significantly positive impact on crop suitability in this region, since no other
 425 factor has such a strong impact on maize suitability. Further south, low precipitation again mostly limits maize suitability.



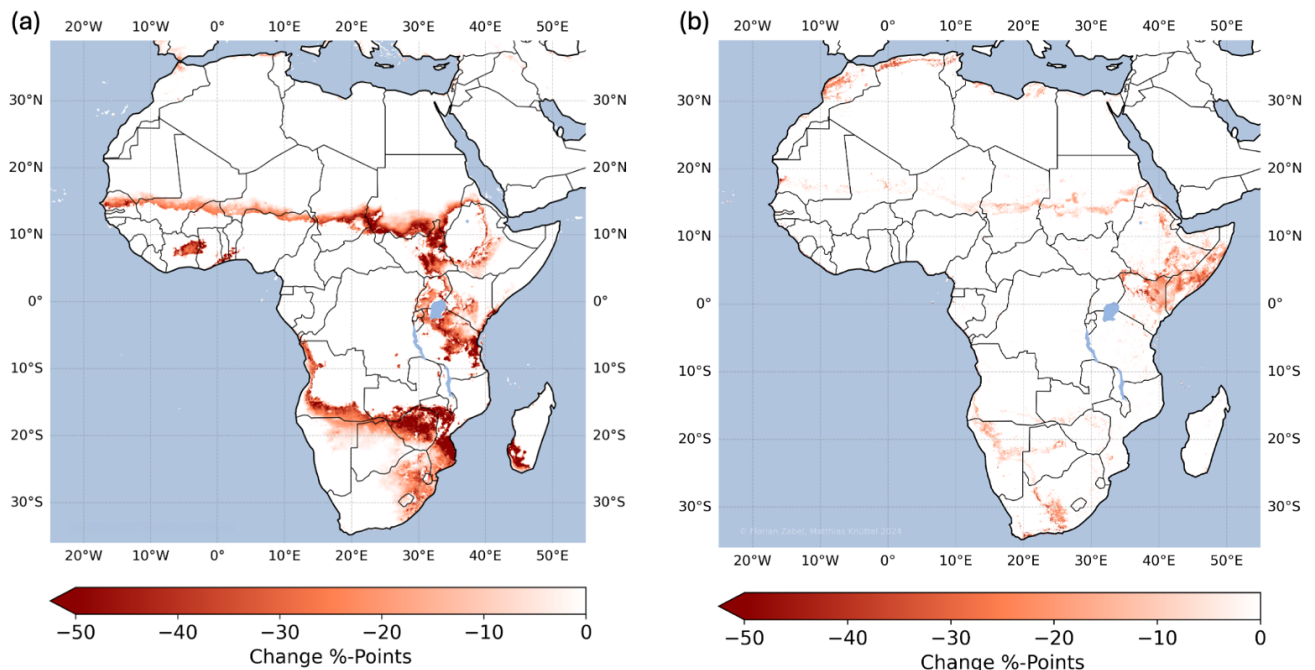
426

427 **Figure 13: Limiting factors.** (a) Most limiting factor of the crop suitability for maize under historical climate conditions from 1991
428 to 2010. (b) shows the degree of limitation of all factors along a transect of the 20° East from 30° North to 30° South. The most limiting
429 factors are displayed with priority according to the order in the legend in (a), if more than one factor fully limits the suitability. For
430 visualization, the shapes in (b) are smoothed using a moving average. Irrigated areas are considered according to Meier et al. (2018)
431 in (a) and are not considered in (b).

432 The consideration of climate variability significantly reduces climate suitability for maize as shown in Fig. 14a, mainly
433 in the transition area between dry savannah and desert in the Sahel zone, in Burundi and Tanzania in Eastern Africa, and
434 in the southern part of Africa in Angola, Zambia, Zimbabwe, Mozambique, South Africa, and the southern part of
435 Madagascar. In total, climate variability reduces climate suitability on more than 5.4 million km².

436 Optimal sowing dates also shift when considering climate variability, since the algorithm identifies the best suitable time
437 window for the growing cycle over the year (Fig. S3710). As a result, optimal sowing for maize considerably shifts in
438 Tanzania, Mozambique and Madagascar.

439 Over all crops, Fig. 14b shows the impact of climate variability on the overall crop suitability. In this case, overall crop
440 suitability is reduced on 2.2 million km², mainly reduced in Somalia, Kenya, Ethiopia, South Africa, and the Maghreb
441 countries of Morocco, Algeria, Tunisia, and Libya. These regions generally show a high vulnerability to climatic
442 variability. Climate variability also reduces the potential for multiple cropping in general over all crops on more than 2.3
443 million km² (Fig. S4811).



444 **Figure 14: Impact of the consideration of climate variability on crop suitability (a) for maize (b) for the overall crop suitability**
445 **of all crops under historical climate conditions from 1991 to 2010.** Irrigated areas are considered according to Meier et al. (2018).
446

447 5 Discussion

448 We found that the consideration of climate variability significantly affects crop suitability, multiple cropping, and optimal
449 sowing dates in Africa. Our approach allows to adjust the risk aversion of farmers by adjusting the thresholds for climate
450 variability (section 2.2.) and the membership function (Fig. 5). The shape of this function may differ between crops and
451 regions and might be influenced by several socio-economic factors, such as the degree of mechanization, financial
452 possibilities, and the availability of crop insurances, which is likely to reduce risk aversion of farmers. We suggest the
453 function as shown in Fig. 5 as a broad and general solution which is primarily designed to represent risk aversion of
454 commercial farms. In our comparison analysis for maize (section 3), ~~reference data showed some cultivation, we were~~
455 ~~able to determine that still agriculture takes place~~ in the regions we identified as unsuitable due to the high recurrence
456 rate of potential crop failures caused by high climate variability (Fig. 7). In some regions, despite the high risk of crop
457 failures, land might be cultivated by smallholders or subsistence farmers that have no other choice but to cultivate these
458 lands. ~~Though~~However, we admit that the tuning of the climate variability thresholds and the membership function
459 requires more research, and the optimal results will vary depending on crop and region. ~~However,~~CropSuite offers the
460 platform and the possibilities to conduct such assessments.

461 The results of CropSuite (section 4) are subject to uncertainties in the applied climate, soil, terrain, and irrigation data as
462 well as the membership functions (Fig. 1). Soil and terrain data are assumed to be static, although management could
463 influence soil properties, such as pH, and terracing could reduce slope limitations. The applied climate data from CHIRPS
464 and CHIRTS are found to be particularly valuable in regions, where climate stations are sparse. Over Africa, CHIRPS is
465 successfully validated (Dinku et al., 2018) showing good performance (Lemma et al., 2019; Muthoni et al., 2019). Verdin
466 et al. (2020) also report good agreement of CHIRTS over Africa, however with a poor performance over central Africa,
467 the Horn of Africa, and parts of northern Mali. Generally, both data sets rely on station data to correct the satellite
468 estimations, which is why uncertainties for very data-scarce regions remain. To apply CropSuite in regions outside 50°S-
469 50°N, or to larger time periods before the 1980s, the user of CropSuite could also rely on global high-resolution climate
470 reanalysis, such as ERA5 (Hersbach et al., 2020). ~~Even though~~ERA5 reanalysis shows large
471 improvements over its predecessor ERA-Interim for the African continent (Gleixner et al., 2020). ~~Still,~~ considerable
472 deviations in precipitation from CHIRPS biases remain are reported, e.g., wet biases over Uganda (Gleixner et al., 2020)
473 and ai (Steinkopf and Engelbrecht, 2022; Terblanche et al., 2022) dry bias over the western Sahel (Gbode et al., 2023),
474 where CHIRPS is applied as reference. We therefore assume that CHIRPS and CHIRTS are very suitable climatic data
475 sets to investigate our example of maize suitability in Africa. The soil profiles used for the generation of the SoilGrids
476 show a heterogeneous distribution, with large gaps over central Africa, which is why Hengl et al. (2017) attribute
477 uncertainty in the data to the under-sampling. They argue that a few hundred additional profiles in under-sampled areas
478 could massively improve the resulting SoilGrids.

479 The membership functions derived by Sys et al. (1993) are widely applied but are also governed by inherent uncertainties.
480 Herzberg et al. (2019) argue that the assessment by Sys et al. (1993) is not detailed enough to capture specific features of
481 small areas. They find that Sys et al. (1993) would consider a hilly area in tropical Vietnam unsuitable due to too acidic
482 soils and steep slopes, whereas the local farmers can cultivate the land. Furthermore, the approach cannot account for
483 compound effects and interactions of the climate and soil variables (Elsheikh et al., 2013). The membership functions
484 cover the general behavior in a univariate manner, while the real plant physiology is a more complex interplay of climatic
485 variables and soil conditions (Joswig et al., 2022). This also applies particularly to compound extremes, for example the
486 combination of hot and dry climatic conditions (Goulart et al., 2023) that limit water availability and favor evaporation,
487 which can trigger water and temperature stress in plants. This is relevant in the course of a warming climate, as the joint
488 probability of hot and dry conditions is projected to increase in many regions of the world (Bevacqua et al., 2022; Felsche
489 et al., 2024). This is however no specific drawback of CropSuite, but rather a lack of bivariate, multivariate or interactive
490 membership functions. The assessment of the membership functions by Sys et al. (1993) is also outdated for new crop
491 varieties that might be more resilient to climatic and environmental stressors (Peter et al., 2020). Furthermore, we argue
492 that the uncertainty in the temperature and precipitation membership functions is by design larger at ~~the~~-its low and high
493 ends, as the functions are derived empirically. Since of the membership function, which affect our consideration of
494 climate variability is based on the 5% to 10% suitability values, respectively (see Section 2.2), the uncertainties of the
495 membership functions are propagated to the assessment of climate variability. More research and updated functions could
496 support the results by CropSuite.

497 The sampling of climate variability within 20-year periods is limited as variability can cover wide time ranges. There,
498 the application of single-model initial condition large ensembles can help to robustly assess the variability based on
499 decadal or multidecadal time periods (Deser et al., 2020). This is especially important for precipitation and precipitation
500 extremes, which show a high sensitivity to climate variability (Lang and Poschlod, 2024; Tebaldi et al., 2021).
501 Furthermore, for the assessment of climate variability, we only capture the occurrence of growing seasons exceeding the
502 percentile thresholds, but we do not consider the intensity of the according events. Single days with extreme precipitation
503 can induce flooding that leads to crop failures (Balgah et al., 2023; Müller et al., 2023), even though the average
504 precipitation for the growing season is still within the suitable range of the membership function. This drawback however
505 also applies for most of the mechanistic crop models at global scale (Ruane et al., 2017), while regional applications
506 evolve incorporating crop losses due to waterlogging and flooding (Li et al., 2016; Monteleone et al., 2023; Pasley et al.,
507 2020). This is why we claim to assess climate variability not climate extremes inducing potential crop failures.

508 **6 Conclusions**

509 CropSuite is a new easy-to-use comprehensive open-source model that provides a complete processing chain
510 (preprocessing, spatial downscaling, suitability simulations, data analysis and visualization) for carrying out crop

511 suitability and climate change impact analysis. CropSuite allows users to easily parameterize different varieties of the
512 same crops or additional crops by determining the membership functions in the GUI. Thereby, the fuzzy logic approach
513 makes it easy to use expert knowledge for the parameterization of the membership functions. Besides all data and
514 compiled maps generated, we provide a user manual for CropSuite (Zabel and Knüttel, 2024) and the parameterizations
515 of the considered 48 crops in this study. Furthermore, the model allows the flexible addition of further parameters and
516 membership functions that might affect suitability, if the required data is provided. For the future, this allows the
517 consideration of further ecological and socio-economic limitations (such as access to fertilizers, available labor, know-
518 how, infrastructure and transportation, heat stress impacts on labor) that have not yet been sufficiently considered in
519 crop suitability assessments (Orlov et al., 2024; Akpoti et al., 2019).

520 For this study, we simulated 48 crops for Africa under the consideration of climate variability for historical climate
521 conditions. Thus, we created a huge dataset, providing detailed high-resolution information on climate-, soil-, and crop
522 suitability, optimal sowing dates, multiple cropping potentials and the limiting factors, which can be used for follow-up
523 studies and climate impact assessments. Additionally, the data include substantial information to develop strategies for
524 an efficient land-use (Schneider et al., 2024; Molina Bacca et al., 2023; Delzeit et al., 2019). The consideration of future
525 climate change scenarios will allow for investigating efficient strategies for climate change adaptation through shifting
526 sowing dates, or cultivar and land-use change. Further, information about the limiting factors can be helpful to optimize
527 crop management, since it identifies the parameter that most efficiently improves crop suitability.

528 **Code Availability**

529 CropSuite (v01.90) code is written in Python and is available Open-Source (CC BY-SA 4.0) together with the GUI ~~and~~
530 ~~a user manual~~ at Zenodo (<https://doi.org/10.5281/zenodo.14259375>) ~~and~~ ~~GitHub~~
531 (<https://github.com/flozabel/CropSuite>). ~~A user manual is provided separately via Zenodo~~
532 (<https://doi.org/10.5281/zenodo.14196315>).

533 **Data Availability**

534 The resulting data are available for download ~~as GeoTIFF files seen via Zenodo~~
535 (<https://doi.org/10.5281/zenodo.14514729>) ~~(10.5281/zenodo.14196331)~~. (~~https://adaptationatlas.cgiar.org~~). In addition to
536 the ~~shown~~ figures ~~shown as examples for maize~~ in this paper, the compiled figures for all 48 ~~considered~~ crops are provided
537 for download, including a separation of rainfed and irrigated agricultural systems and a comparison with MapSPAM
538 2020 (~~https://doi.org/10.5281/zenodo.14514729~~(~~10.5281/zenodo.14196331~~)).

539 **Author contribution**

540 FZ conceptualized and developed the model. MK programmed the CropSuite model and the GUI in Python. FZ, MK,
541 and BP developed the methodology for the consideration of climate variability. FZ and MK performed the simulations
542 and analyzed the results. FZ and MK prepared the manuscript with contributions from BP.

543 **Competing interests**

544 The authors declare that they have no conflict of interest.

545 **Acknowledgements**

546 The simulations were performed at sciCORE (<http://scicore.unibas.ch/>) scientific computing center at University of
547 Basel, requiring in total approximately 150.000 CPUh. We thank CGIAR and CIAT for their support and the scholarship
548 provided to MK and the collaboration for the Africa Agriculture Adaptation Atlas.

549 **References**

- 550 Abdulai, A. L., Kouressy, M., Vaksman, M., Asch, F., Giese, M., and Holger, B.: Latitude and Date of Sowing
551 Influences Phenology of Photoperiod-Sensitive Sorghums, *Journal of Agronomy and Crop Science*, 198, 340-348,
552 10.1111/j.1439-037X.2012.00523.x, 2012.
- 553 Akpoti, K., Kabo-bah, A. T., and Zwart, S. J.: Review - Agricultural land suitability analysis: State-of-the-art and outlooks
554 for integration of climate change analysis, *Agricultural Systems*, 173, 172-208,
555 <https://doi.org/10.1016/j.agsy.2019.02.013>, 2019.
- 556 Akpoti, K., Kabo-bah, A. T., Dossou-Yovo, E. R., Groen, T. A., and Zwart, S. J.: Mapping suitability for rice production
557 in inland valley landscapes in Benin and Togo using environmental niche modeling, *Science of The Total*
558 *Environment*, 709, 136165, <https://doi.org/10.1016/j.scitotenv.2019.136165>, 2020.
- 559 Asseng, S., Spänkuch, D., Hernandez-Ochoa, I. M., and Laporta, J.: The upper temperature thresholds of life, *The Lancet*
560 *Planetary Health*, 5, e378-e385, [https://doi.org/10.1016/S2542-5196\(21\)00079-6](https://doi.org/10.1016/S2542-5196(21)00079-6), 2021.
- 561 Avellan, T., Zabel, F., and Mauser, W.: The influence of input data quality in determining areas suitable for crop growth
562 at the global scale – a comparative analysis of two soil and climate datasets, *Soil Use and Management*, 28, 249-265,
563 <https://doi.org/10.1111/j.1475-2743.2012.00400.x>, 2012.
- 564 Balgah, R. A., Ngwa, K. A., Buchenrieder, G. R., and Kimengsi, J. N.: Impacts of Floods on Agriculture-Dependent
565 Livelihoods in Sub-Saharan Africa: An Assessment from Multiple Geo-Ecological Zones, *Land*, 12, 334, 2023.
- 566 Batjes, N. H.: Harmonized soil property values for broad-scale modelling (WISE30sec) with estimates of global soil
567 carbon stocks, *Geoderma*, 269, 61-68, <https://doi.org/10.1016/j.geoderma.2016.01.034>, 2016.
- 568 Bevacqua, E., Zappa, G., Lehner, F., and Zscheischler, J.: Precipitation trends determine future occurrences of compound
569 hot-dry events, *Nat Clim Change*, 12, 350-355, 10.1038/s41558-022-01309-5, 2022.
- 570 Bonfante, A., Monaco, E., Alfieri, S. M., De Lorenzi, F., Manna, P., Basile, A., and Bouma, J.: Chapter Two - Climate
571 Change Effects on the Suitability of an Agricultural Area to Maize Cultivation: Application of a New Hybrid Land
572 Evaluation System, in: *Advances in Agronomy*, edited by: Sparks, D. L., Academic Press, 33-69,
573 <https://doi.org/10.1016/bs.agron.2015.05.001>, 2015.

574 Chapman, S., E Birch, C., Pope, E., Sallu, S., Bradshaw, C., Davie, J., and H Marsham, J.: Impact of climate change on
575 crop suitability in sub-Saharan Africa in parameterized and convection-permitting regional climate models,
576 Environmental Research Letters, 15, 094086, 10.1088/1748-9326/ab9daf, 2020.

577 Chemura, A., Gleixner, S., and Gornott, C.: Dataset of the suitability of major food crops in Africa under climate change,
578 Scientific Data, 11, 294, 10.1038/s41597-024-03118-1, 2024.

579 Chen, D., Dai, A., and Hall, A.: The Convective-To-Total Precipitation Ratio and the “Drizzling” Bias in Climate Models,
580 Journal of Geophysical Research: Atmospheres, 126, e2020JD034198, <https://doi.org/10.1029/2020JD034198>, 2021.

581 Cober, E. R. and Morrison, M. J.: Regulation of seed yield and agronomic characters by photoperiod sensitivity and
582 growth habit genes in soybean, Theoretical and Applied Genetics, 120, 1005-1012, 10.1007/s00122-009-1228-6,
583 2010.

584 Cronin, J., Zabel, F., Dessens, O., and Anandarajah, G.: Land suitability for energy crops under scenarios of climate
585 change and land-use, GCB Bioenergy, 12, 648–665-648–665, <https://doi.org/10.1111/gcbb.12697>, 2020.

586 Daly, C., Neilson, R. P., and Phillips, D. L.: A Statistical-Topographic Model for Mapping Climatological Precipitation
587 over Mountainous Terrain, Journal of Applied Meteorology and Climatology, 33, 140-158,
588 [https://doi.org/10.1175/1520-0450\(1994\)033<0140:ASTMFM>2.0.CO;2](https://doi.org/10.1175/1520-0450(1994)033<0140:ASTMFM>2.0.CO;2), 1994.

589 Damiani, A., Ishizaki, N. N., Sasaki, H., Feron, S., and Cordero, R. R.: Exploring super-resolution spatial downscaling
590 of several meteorological variables and potential applications for photovoltaic power, Scientific Reports, 14, 7254,
591 10.1038/s41598-024-57759-8, 2024.

592 Delzeit, R., Pongratz, J., Schneider, J. M., Schuenemann, F., Mauser, W., and Zabel, F.: Forest restoration: Expanding
593 agriculture, Science, 366, 316–317-316–317, <https://doi.org/10.1126/science.aaz0705>, 2019.

594 Deser, C., Lehner, F., Rodgers, K. B., Ault, T., Delworth, T. L., DiNezio, P. N., Fiore, A., Frankignoul, C., Fyfe, J. C.,
595 Horton, D. E., Kay, J. E., Knutti, R., Lovenduski, N. S., Marotzke, J., McKinnon, K. A., Minobe, S., Randerson, J.,
596 Screen, J. A., Simpson, I. R., and Ting, M.: Insights from Earth system model initial-condition large ensembles and
597 future prospects, Nat Clim Change, 10, 277-286, 10.1038/s41558-020-0731-2, 2020.

598 Dewitte, O., Jones, A., Spaargaren, O., Breuning-Madsen, H., Brossard, M., Dampha, A., Deckers, J., Gallali, T., Hallett,
599 S., Jones, R., Kilasara, M., Le Roux, P., Michéli, E., Montanarella, L., Thiombiano, L., Van Ranst, E., Yemefack, M.,
600 and Zougmore, R.: Harmonisation of the soil map of Africa at the continental scale, Geoderma, 211-212, 138-153,
601 <https://doi.org/10.1016/j.geoderma.2013.07.007>, 2013.

602 Dinku, T., Funk, C., Peterson, P., Maidment, R., Tadesse, T., Gadain, H., and Ceccato, P.: Validation of the CHIRPS
603 satellite rainfall estimates over eastern Africa, Quarterly Journal of the Royal Meteorological Society, 144, 292-312,
604 <https://doi.org/10.1002/qj.3244>, 2018.

605 Elsheikh, R., Mohamed Shariff, A. R. B., Amiri, F., Ahmad, N. B., Balasundram, S. K., and Soom, M. A. M.: Agriculture
606 Land Suitability Evaluator (ALSE): A decision and planning support tool for tropical and subtropical crops, Comput
607 Electron Agr, 93, 98-110, <https://doi.org/10.1016/j.compag.2013.02.003>, 2013.

608 FAO: The Ecocrop Database [dataset], 2024.

609 FAO, IIASA, ISRIC, ISSCAS, and JRC: Harmonized World Soil Database (version 1.2) [dataset], 2012.

610 Farr, T. G., Rosen, P. A., Caro, E., Crippen, R., Duren, R., Hensley, S., Kobrick, M., Paller, M., Rodriguez, E., Roth, L.,
611 Seal, D., Shaffer, S., Shimada, J., Umland, J., Werner, M., Oskin, M., Burbank, D., and Alsdorf, D.: The Shuttle
612 Radar Topography Mission, Reviews of Geophysics, 45, RG2004, 10.1029/2005RG000183, 2007.

613 Felsche, E., Böhnisch, A., Poschlod, B., and Ludwig, R.: European hot and dry summers are projected to become more
614 frequent and expand northwards, Communications Earth & Environment, 5, 410, 10.1038/s43247-024-01575-5,
615 2024.

616 Fick, S. E. and Hijmans, R. J.: WorldClim 2: new 1-km spatial resolution climate surfaces for global land areas,
617 International Journal of Climatology, 37, 4302-4315, 10.1002/joc.5086, 2017.

618 Fiddes, J., Aalstad, K., and Lehning, M.: TopoCLIM: rapid topography-based downscaling of regional climate model
619 output in complex terrain v1.1, Geosci. Model Dev., 15, 1753-1768, 10.5194/gmd-15-1753-2022, 2022.

620 Fischer, G., Nachtergaele, F. O., van Velthuizen, H. T., Chiozza, F., Franceschini, G., Henry, M., Muchoney, D., and
621 Tramberend, S.: Global Agro-Ecological Zones v4 - Model documentation, 1, FAO, Rome,
622 <https://doi.org/10.4060/cb4744en>, 2021.

623 Franke, J. A., Müller, C., Minoli, S., Elliott, J., Folberth, C., Gardner, C., Hank, T., Izaurralde, R. C., Jägermeyr, J., Jones,
624 C. D., Liu, W., Olin, S., Pugh, T. A. M., Ruane, A. C., Stephens, H., Zabel, F., and Moyer, E. J.: Agricultural
625 breadbaskets shift poleward given adaptive farmer behavior under climate change, *Global Change Biol*, 28, 167–181–
626 167–181, <https://doi.org/10.1111/gcb.15868>, 2021.

627 Funk, C., Peterson, P., Landsfeld, M., Pedreros, D., Verdin, J., Shukla, S., Husak, G., Rowland, J., Harrison, L., Hoell,
628 A., and Michaelsen, J.: The climate hazards infrared precipitation with stations—a new environmental record for
629 monitoring extremes, *Scientific Data*, 2, 150066, 10.1038/sdata.2015.66, 2015.

630 Funk, C., Peterson, P., Peterson, S., Shukla, S., Davenport, F., Michaelsen, J., Knapp, K. R., Landsfeld, M., Husak, G.,
631 Harrison, L., Rowland, J., Budde, M., Meiburg, A., Dinku, T., Pedreros, D., and Mata, N.: A High-Resolution 1983–
632 2016 Tmax Climate Data Record Based on Infrared Temperatures and Stations by the Climate Hazard Center, *Journal*
633 *of Climate*, 32, 5639–5658, <https://doi.org/10.1175/JCLI-D-18-0698.1>, 2019.

634 Gbode, I. E., Babalola, T. E., Diro, G. T., and Intsiful, J. D.: Assessment of ERA5 and ERA-Interim in Reproducing
635 Mean and Extreme Climates over West Africa, *Advances in Atmospheric Sciences*, 40, 570–586, 10.1007/s00376-
636 022-2161-8, 2023.

637 Gleixner, S., Demissie, T., and Diro, G. T.: Did ERA5 Improve Temperature and Precipitation Reanalysis over East
638 Africa?, *Atmosphere*, 11, 996, 2020.

639 Goulart, H. M. D., van der Wiel, K., Folberth, C., Balkovic, J., and van den Hurk, B.: Storylines of weather-induced crop
640 failure events under climate change, *Earth Syst. Dynam.*, 12, 1503–1527, 10.5194/esd-12-1503-2021, 2021.

641 Goulart, H. M. D., van der Wiel, K., Folberth, C., Boere, E., and van den Hurk, B.: Increase of Simultaneous Soybean
642 Failures Due To Climate Change, *Earth's Future*, 11, e2022EF003106, <https://doi.org/10.1029/2022EF003106>, 2023.

643 Hengl, T., de Jesus, J. M., MacMillan, R. A., Batjes, N. H., Heuvelink, G. B. M., Ribeiro, E., Samuel-Rosa, A., Kempen,
644 B., Leenaars, J. G. B., Walsh, M. G., and Gonzalez, M. R.: SoilGrids1km — Global Soil Information Based on
645 Automated Mapping, *PLOS ONE*, 9, e105992, 10.1371/journal.pone.0105992, 2014.

646 Hengl, T., Mendes de Jesus, J., Heuvelink, G. B. M., Ruiperez Gonzalez, M., Kilibarda, M., Blagotić, A., Shangguan,
647 W., Wright, M. N., Geng, X., Bauer-Marschallinger, B., Guevara, M. A., Vargas, R., MacMillan, R. A., Batjes, N.
648 H., Leenaars, J. G. B., Ribeiro, E., Wheeler, I., Mantel, S., and Kempen, B.: SoilGrids250m: Global gridded soil
649 information based on machine learning, *PLOS ONE*, 12, e0169748, 10.1371/journal.pone.0169748, 2017.

650 Hersbach, H., Bell, B., Berrisford, P., Hirahara, S., Horányi, A., Muñoz-Sabater, J., Nicolas, J., Peubey, C., Radu, R.,
651 Schepers, D., Simmons, A., Soci, C., Abdalla, S., Abellan, X., Balsamo, G., Bechtold, P., Biavati, G., Bidlot, J.,
652 Bonavita, M., De Chiara, G., Dahlgren, P., Dee, D., Diamantakis, M., Dragani, R., Flemming, J., Forbes, R., Fuentes,
653 M., Geer, A., Haimberger, L., Healy, S., Hogan, R. J., Hólm, E., Janisková, M., Keeley, S., Laloyaux, P., Lopez, P.,
654 Lupu, C., Radnoti, G., de Rosnay, P., Rozum, I., Vamborg, F., Villaume, S., and Thépaut, J.-N.: The ERA5 global
655 reanalysis, *Quarterly Journal of the Royal Meteorological Society*, 146, 1999–2049, <https://doi.org/10.1002/qj.3803>,
656 2020.

657 Herzberg, R., Pham, T. G., Kappas, M., Wyss, D., and Tran, C. T. M.: Multi-Criteria Decision Analysis for the Land
658 Evaluation of Potential Agricultural Land Use Types in a Hilly Area of Central Vietnam, *Land*, 8, 90, 2019.

659 IFPRI: Global Spatially-Disaggregated Crop Production Statistics Data for 2020 Version 1.0, Harvard Dataverse
660 [dataset], <https://doi.org/10.7910/DVN/SWPENT>, 2024.

661 IPCC: Climate Change 2021: The Physical Science Basis. Contribution of Working Group I to the Sixth Assessment
662 Report of the Intergovernmental Panel on Climate Change, Cambridge University Press, 2021.

663 Ivushkin, K., Bartholomeus, H., Bregt, A. K., Pulatov, A., Kempen, B., and de Sousa, L.: Global mapping of soil salinity
664 change, *Remote Sens Environ*, 231, 111260, <https://doi.org/10.1016/j.rse.2019.111260>, 2019.

665 Jägermeyr, J., Robock, A., Elliott, J., Müller, C., Xia, L., Khabarov, N., Folberth, C., Schmid, E., Liu, W., Zabel, F.,
666 Rabin, S. S., Puma, M. J., Heslin, A., Franke, J., Foster, I., Asseng, S., Bardeen, C. G., Toon, O. B., and Rosenzweig,
667 C.: A regional nuclear conflict would compromise global food security, *Proceedings of the National Academy of*
668 *Sciences*, 117, 7071–7081–7071–7081, <https://doi.org/10.1073/pnas.1919049117>, 2020.

669 Jägermeyr, J., Müller, C., Ruane, A. C., Elliott, J., Balkovic, J., Castillo, O., Faye, B., Foster, I., Folberth, C., Franke, J.
670 A., Fuchs, K., Guarin, J. R., Heinke, J., Hoogenboom, G., Iizumi, T., Jain, A. K., Kelly, D., Khabarov, N., Lange, S.,
671 Lin, T.-S., Liu, W., Mialyk, O., Minoli, S., Moyer, E. J., Okada, M., Phillips, M., Porter, C., Rabin, S. S., Scheer, C.,
672 Schneider, J. M., Schyns, J. F., Skalsky, R., Smerald, A., Stella, T., Stephens, H., Webber, H., Zabel, F., and

673 Rosenzweig, C.: Climate impacts on global agriculture emerge earlier in new generation of climate and crop models,
674 Nature Food, 2, 873–885-873–885, <https://doi.org/10.1038/s43016-021-00400-y>, 2021.

675 Joswig, J. S., Wirth, C., Schuman, M. C., Kattge, J., Reu, B., Wright, I. J., Sippel, S. D., Rüger, N., Richter, R.,
676 Schaepman, M. E., van Bodegom, P. M., Cornelissen, J. H. C., Diaz, S., Hatttingh, W. N., Kramer, K., Lens, F.,
677 Niinemets, Ü., Reich, P. B., Reichstein, M., Römermann, C., Schrodt, F., Anand, M., Bahn, M., Byun, C., Campetella,
678 G., Cerabolini, B. E. L., Craine, J. M., Gonzalez-Melo, A., Gutiérrez, A. G., He, T., Higuchi, P., Jactel, H., Kraft, N.
679 J. B., Minden, V., Onipchenko, V., Peñuelas, J., Pillar, V. D., Sosinski, Ê., Soudzilovskaia, N. A., Weiher, E., and
680 Mahecha, M. D.: Climatic and soil factors explain the two-dimensional spectrum of global plant trait variation, Nature
681 Ecology & Evolution, 6, 36-50, 10.1038/s41559-021-01616-8, 2022.

682 Karger, D. N., Lange, S., Hari, C., Reyer, C. P. O., Conrad, O., Zimmermann, N. E., and Frieler, K.: CHELSA-W5E5:
683 daily 1 km meteorological forcing data for climate impact studies, Earth Syst. Sci. Data, 15, 2445-2464,
684 10.5194/essd-15-2445-2023, 2023.

685 Karl, K., MacCarthy, D., Porciello, J., Chimwaza, G., Fredenberg, E., Freduah, B. S., Guarin, J., Mendez Leal, E.,
686 Kozlowski, N., Narh, S., Sheikh, H., Valdivia, R., Wesley, G., Van Deynze, A., van Zonneveld, M., and Yang, M.:
687 Opportunity Crop Profiles for the Vision for Adapted Crops and Soils (VACS) in Africa,
688 <https://doi.org/10.7916/7msa-yy32>, 2024.

689 Knüttel, M. and Zabel, F.: CropSuite User Manual, <https://doi.org/10.5281/zenodo.14196315>, 2024.

690 Lang, A. and Poschlo, B.: Updating catastrophe models to today's climate – An application of a large ensemble approach
691 to extreme rainfall, Climate Risk Management, 44, 100594, <https://doi.org/10.1016/j.crm.2024.100594>, 2024.

692 Lemma, E., Upadhyaya, S., and Ramsankaran, R.: Investigating the performance of satellite and reanalysis rainfall
693 products at monthly timescales across different rainfall regimes of Ethiopia, International Journal of Remote Sensing,
694 40, 4019-4042, 10.1080/01431161.2018.1558373, 2019.

695 Li, S., Tompkins, A. M., Lin, E., and Ju, H.: Simulating the impact of flooding on wheat yield – Case study in East China,
696 Agr Forest Meteorol, 216, 221-231, <https://doi.org/10.1016/j.agrformet.2015.10.014>, 2016.

697 Maleki, F., Kazemi, H., Siahmarguee, A., and Kamkar, B.: Development of a land use suitability model for saffron
698 (*Crocus sativus* L.) cultivation by multi-criteria evaluation and spatial analysis, Ecol Eng, 106, 140-153,
699 <https://doi.org/10.1016/j.ecoleng.2017.05.050>, 2017.

700 Marke, T., Mauser, W., Pfeiffer, A., Zängl, G., Jacob, D., and Strasser, U.: Application of a hydrometeorological model
701 chain to investigate the effect of global boundaries and downscaling on simulated river discharge, Environ Earth Sci,
702 71, 4849-4868, 10.1007/s12665-013-2876-z, 2014.

703 Meier, J., Zabel, F., and Mauser, W.: A global approach to estimate irrigated areas – a comparison between different data
704 and statistics, Hydrology and Earth System Sciences, 22, 1119–1133-1119–1133, 2018.

705 Molina Bacca, E. J., Stevanović, M., Bodirsky, B. L., Karstens, K., Chen, D. M.-C., Leip, D., Müller, C., Minoli, S.,
706 Heinke, J., Jägermeyr, J., Folberth, C., Iizumi, T., Jain, A. K., Liu, W., Okada, M., Smerald, A., Zabel, F., Lotze-
707 Campen, H., and Popp, A.: Uncertainty in land-use adaptation persists despite crop model projections showing lower
708 impacts under high warming, Communications Earth & Environment, 4, 284, 10.1038/s43247-023-00941-z, 2023.

709 Monteleone, B., Giusti, R., Magnini, A., Arosio, M., Domeneghetti, A., Borzi, I., Petruccelli, N., Castellarin, A.,
710 Bonaccorso, B., and Martina, M. L. V.: Estimations of Crop Losses Due to Flood Using Multiple Sources of
711 Information and Models: The Case Study of the Panaro River, Water, 15, 1980, 2023.

712 Müller, C., Ouédraogo, W. A., Schwarz, M., Barteit, S., and Sauerborn, R.: The effects of climate change-induced
713 flooding on harvest failure in Burkina Faso: case study, Frontiers in Public Health, 11, 10.3389/fpubh.2023.1166913,
714 2023.

715 Müller, C., Jägermeyr, J., Franke, J. A., Ruane, A. C., Balkovic, J., Ciais, P., Dury, M., Falloon, P., Folberth, C., Hank,
716 T., Hoffmann, M., Izaurralde, R. C., Jacquemin, I., Khabarov, N., Liu, W., Olin, S., Pugh, T. A. M., Wang, X.,
717 Williams, K., Zabel, F., and Elliott, J. W.: Substantial Differences in Crop Yield Sensitivities Between Models Call
718 for Functionality-Based Model Evaluation, Earth's Future, 12, e2023EF003773,
719 <https://doi.org/10.1029/2023EF003773>, 2024.

720 Muthoni, F. K., Odongo, V. O., Ochieng, J., Mugalavai, E. M., Mourice, S. K., Hoesche-Zeledon, I., Mwila, M., and
721 Bekunda, M.: Long-term spatial-temporal trends and variability of rainfall over Eastern and Southern Africa,
722 Theoretical and Applied Climatology, 137, 1869-1882, 10.1007/s00704-018-2712-1, 2019.

723 Orlov, A., Jägermeyr, J., Müller, C., Daloz, A. S., Zabel, F., Minoli, S., Liu, W., Lin, T.-S., Jain, A. K., Folberth, C.,
724 Okada, M., Poschlod, B., Smerald, A., Schneider, J. M., and Sillmann, J.: Human heat stress could offset potential
725 economic benefits of CO₂ fertilization in crop production under a high-emissions scenario, *One Earth*, 7, 1250-1265,
726 <https://doi.org/10.1016/j.oneear.2024.06.012>, 2024.

727 Pasley, H. R., Huber, I., Castellano, M. J., and Archontoulis, S. V.: Modeling Flood-Induced Stress in Soybeans, *Frontiers*
728 *in Plant Science*, 11, 10.3389/fpls.2020.00062, 2020.

729 Pelletier, J. D., Broxton, P. D., Hazenberg, P., Zeng, X., Troch, P. A., Niu, G.-Y., Williams, Z., Brunke, M. A., and
730 Gochis, D.: A gridded global data set of soil, intact regolith, and sedimentary deposit thicknesses for regional and
731 global land surface modeling, *Journal of Advances in Modeling Earth Systems*, 8, 41-65,
732 <https://doi.org/10.1002/2015MS000526>, 2016.

733 Peter, B. G., Messina, J. P., Lin, Z., and Snapp, S. S.: Crop climate suitability mapping on the cloud: a geovisualization
734 application for sustainable agriculture, *Scientific Reports*, 10, 15487, 10.1038/s41598-020-72384-x, 2020.

735 Ramirez-Villegas, J., Jarvis, A., and Läderach, P.: Empirical approaches for assessing impacts of climate change on
736 agriculture: The EcoCrop model and a case study with grain sorghum, *Agr Forest Meteorol*, 170, 67-78,
737 <https://doi.org/10.1016/j.agrformet.2011.09.005>, 2013.

738 Ranjitkar, S., Sujakhu, N. M., Merz, J., Kindt, R., Xu, J., Matin, M. A., Ali, M., and Zomer, R. J.: Suitability Analysis
739 and Projected Climate Change Impact on Banana and Coffee Production Zones in Nepal, *PLOS ONE*, 11, e0163916,
740 10.1371/journal.pone.0163916, 2016.

741 Ruane, A. C., Rosenzweig, C., Asseng, S., Boote, K. J., Elliott, J., Ewert, F., Jones, J. W., Martre, P., McDermid, S. P.,
742 Müller, C., Snyder, A., and Thorburn, P. J.: An AgMIP framework for improved agricultural representation in
743 integrated assessment models, *Environmental Research Letters*, 12, 125003, 10.1088/1748-9326/aa8da6, 2017.

744 Schneider, J. M., Zabel, F., and Mauser, W.: Global inventory of suitable, cultivable and available cropland under
745 different scenarios and policies, *Scientific Data*, 9, <https://doi.org/10.1038/s41597-022-01632-8>, 2022a.

746 Schneider, J. M., Zabel, F., and Mauser, W.: Global inventory of suitable, cultivable and available cropland under
747 different scenarios and policies, *Scientific Data*, 9, 527, 10.1038/s41597-022-01632-8, 2022b.

748 Schneider, J. M., Delzeit, R., Neumann, C., Heimann, T., Seppelt, R., Schuenemann, F., Söder, M., Mauser, W., and
749 Zabel, F.: Effects of profit-driven cropland expansion and conservation policies, *Nature Sustainability*, 7, 1335-1347,
750 10.1038/s41893-024-01410-x, 2024.

751 Steinkopf, J. and Engelbrecht, F.: Verification of ERA5 and ERA-Interim precipitation over Africa at intra-annual and
752 interannual timescales, *Atmospheric Research*, 280, 106427, <https://doi.org/10.1016/j.atmosres.2022.106427>, 2022.

753 Sun, Y., Solomon, S., Dai, A., and Portmann, R. W.: How Often Does It Rain?, *Journal of Climate*, 19, 916-934,
754 10.1175/jcli3672.1, 2006.

755 Sys, C. O., van Ranst, E., and Debaveye, J.: Land evaluation: Part II Methods in Land Evaluation, G.A.D.C, Brussels,
756 1991.

757 Sys, C. O., van Ranst, E., Debaveye, J., and Beernaert, F.: Land evaluation: Part III Crop requirements, G.A.D.C,
758 Brussels, 1993.

759 Tebaldi, C., Dorheim, K., Wehner, M., and Leung, R.: Extreme metrics from large ensembles: investigating the effects
760 of ensemble size on their estimates, *Earth Syst. Dynam.*, 12, 1427-1501, 10.5194/esd-12-1427-2021, 2021.

761 Terblanche, D., Lynch, A., Chen, Z., and Sinclair, S.: ERA5-Derived Precipitation: Insights from Historical Rainfall
762 Networks in Southern Africa, *Journal of Applied Meteorology and Climatology*, 61, 1473-1484,
763 <https://doi.org/10.1175/JAMC-D-21-0096.1>, 2022.

764 van Zonneveld, M., Kindt, R., McMullin, S., Achigan-Dako, E. G., N'Danikou, S., Hsieh, W.-h., Lin, Y.-r., and Dawson,
765 I. K.: Forgotten food crops in sub-Saharan Africa for healthy diets in a changing climate, *Proceedings of the National*
766 *Academy of Sciences*, 120, e2205794120, 10.1073/pnas.2205794120, 2023.

767 Verdin, A., Funk, C., Peterson, P., Landsfeld, M., Tuholske, C., and Grace, K.: Development and validation of the
768 CHIRTS-daily quasi-global high-resolution daily temperature data set, *Scientific Data*, 7, 303, 10.1038/s41597-020-
769 00643-7, 2020.

770 Vogel, E., Donat, M. G., Alexander, L. V., Meinshausen, M., Ray, D. K., Karoly, D., Meinshausen, N., and Frieler, K.:
771 The effects of climate extremes on global agricultural yields, *Environmental Research Letters*, 14, 054010,
772 10.1088/1748-9326/ab154b, 2019.

773 Wang, F., Tian, D., Lowe, L., Kalin, L., and Lehrter, J.: Deep Learning for Daily Precipitation and Temperature
774 Downscaling, *Water Resources Research*, 57, e2020WR029308, <https://doi.org/10.1029/2020WR029308>, 2021.

775 Yu, Q., You, L., Wood-Sichra, U., Ru, Y., Joglekar, A. K. B., Fritz, S., Xiong, W., Lu, M., Wu, W., and Yang, P.: A
776 cultivated planet in 2010 – Part 2: The global gridded agricultural-production maps, *Earth Syst. Sci. Data*, 12, 3545-
777 3572, 10.5194/essd-12-3545-2020, 2020.

778 Zabel, F.: Global Agricultural Land Resources – A High Resolution Suitability Evaluation and Its Perspectives until 2100
779 under Climate Change Conditions (v3.0) Zenodo [dataset], <https://doi.org/10.5281/zenodo.5982577>, 2022.

780 Zabel, F. and Knüttel, M.: CropSuite Version 1.0 User Manual, 21.05.2024.

781 Zabel, F., Putzenlechner, B., and Mauser, W.: Global Agricultural Land Resources – A High Resolution Suitability
782 Evaluation and Its Perspectives until 2100 under Climate Change Conditions, *PLoS ONE*, 9, e107522-e107522,
783 <https://doi.org/10.1371/journal.pone.0107522>, 2014.

784